Analysis of NRC/IOT marine dynamics test facility

Booton, M.

Publisher's version / Version de l'éditeur:
https://doi.org/10.4224/8895666
Contractor Report (National Research Council of Canada. Institute for Ocean Technology); no. CR-2007-01, 2007-06-01

National Research Council Canada
Conseil national de recherches Canada

Institute for Ocean Technology
Institut des technologies océaniques

CR-2007-01

ANALYSIS OF NRC/IOT MARINE DYNAMICS TEST FACILITY

M. Booton

June 2007

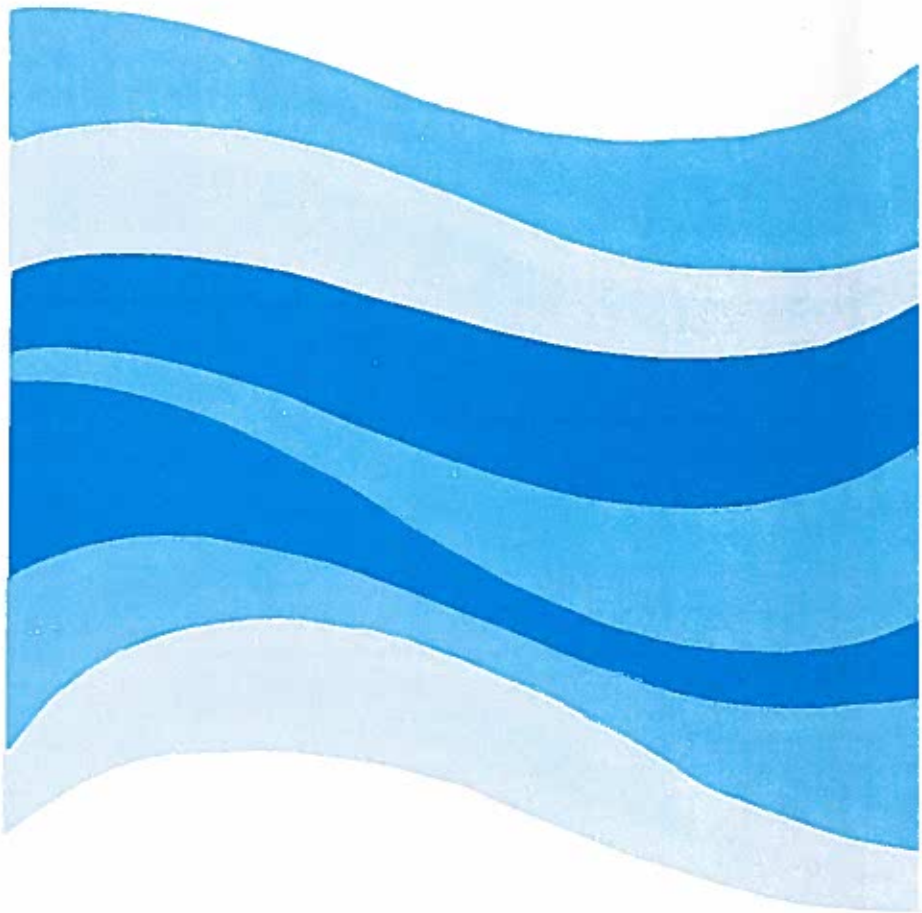

Canada

DOCUMENTATION PAGE

REPORT NUMBER	NRC REPORT NUMBER	DATE
CR-2007-01		June 2007
REPORT SECURITY CLASSIFICATION		**DISTRIBUTION**
Unclassified		Unlimited

TITLE

ANALYSIS OF NRC/IOT MARINE DYNAMICS TEST FACILITY

AUTHOR(S)

M. Booton

CORPORATE AUTHOR(S)/PERFORMING AGENCY(S)

Institute for Ocean Technology, National Research Council, St. John's, NL

PUBLICATION

SPONSORING AGENCY(S)

Memorial University, Faculty of Engineering and Applied Science, St. John's, NL

IOT PROJECT NUMBER	NRC FILE NUMBER

KEY WORDS	PAGES	FIGS.	TABLES
MDTF, struts, dynamometer, carriage, sting	22	25	

SUMMARY

During tests of marine vehicles, there are a number of issues regarding the operation of the National Research Council of Canada, Institute for Ocean Technology, Marine Dynamics Test Facility (NRC/IOTMDTF). The objective was to provide information re-garding the structural dynamic behaviour of the system. This report presents results of the following analyses.

- Natural frequencies for various model/sting configurations for various strut extensions sizes, yaw angles and pitch angles calculated using a finite element idealization of the system.
- Linear static FE analysis of the Albert model for the case of zero pitch and yaw, both struts fully extended for different unit load cases in six degrees of freedom.
- Dynamic response estimates of the Albert model for a harmonics way test, with both struts fully extended for different towing speeds, input amplitudes and input frequencies using a mathematical model for the equation of motion of the model, taking into account the flexibility of the system. Estimates of loading on the MDTF were obtained.
- Dynamic response estimates of the DSUB model for a harmonics way test for different towing speeds, input amplitudes and input frequencies using a mathematical model for the equation of motion of the model, taking into account the flexibility of the system. These estimates were compared with test results.
- Sting lateral and angular deflections at the model BRC, forward yoke and aft yoke locations due to a unit side force and unity awing moment applied to the model BRC. These results were obtained for the purpose of providing corrections to yaw angle in a steady yaw test.

ADDRESS National Research Council
Institute for Ocean Technology
Arctic Avenue, P. O. Box 12093
St. John's, NL A1B 3T5
Tel.: (709) 772-5185, Fax: (709) 772-2462

National Research Council Canada
Institute for Ocean Technology

Conseil national de recherches Canada
Institut des technologies océaniques

ANALYSIS OF NRC/IOT MARINE DYNAMICS TEST FACILITY

CR-2007-01

M. Booton

June 2007

Analysis of NRC/IOT Marine Dynamics Test Facility

M. Booton
Ph.D., P.Eng.

March, 2006

Contents

Summary

During tests of marine vehicles, there are a number of issues regarding the operation of the National Research Council of Canada, Institute for Ocean Technology, Marine Dynamics Test Facility (NRC/IOT MDTF). The objective was to provide information regarding the structural dynamic behaviour of the system. This report presents results of the following analyses.

- Natural frequencies for various model/sting configurations for various strut extensions sizes, yaw angles and pitch angles calculated using a finite element idealization of the system.
- Linear static FE analysis of the Albert model for the case of zero pitch and yaw, both struts fully extended for different unit load cases in six degrees of freedom.
- Dynamic response estimates of the Albert model for a harmonic sway test, with both struts fully extended for different towing speeds, input amplitudes and input frequencies using a mathematical model for the equation of motion of the model, taking into account the flexibility of the system. Estimates of loading on the MDTF were obtained.
- Dynamic response estimates of the DSUB model for a harmonic sway test for different towing speeds, input amplitudes and input frequencies using a mathematical model for the equation of motion of the model, taking into account the flexibility of the system. These estimates were compared with test results.
- Sting lateral and angular deflections at the model BRC, forward yoke and aft yoke locations due to a unit side force and unit yawing moment applied to the model BRC. These results were obtained for the purpose of providing corrections to yaw angle in a steady yaw test.

Acknowledgments

This report was based on information provided by the National Research Council of Canada Institute for Ocean Technology (NRC/IOT). Engineering data, drawings and other data were provided by John Bell. Hydrodynamic data, test records and other information were obtained from Christopher Williams. Michael Sullivan provided test data for the purpose of estimating damping factors. Michael MacKay of DRDC (Defence Research & Development Canada – Atlantic) provided added mass properties and hydrodynamic data.

Introduction and Background

Description of MDTF

The MDTF is a 6 degree of freedom motion generation system installed on the towing carriage of the 200 m x 12 m x 7 m clearwater tank at NRC/IOT. The facility allows the movement of a captive model of an underwater vehicle such as a submarine or a surface model in any simultaneous combination of heave, pitch, sway and yaw by means of computer-controlled electric servo actuators, as shown in Figure 1. A submerged vehicle is typically sting-mounted at the tail, to provide minimal intrusion. Submarine models up to 6 m in length can be accommodated. The towing carriage has a maximum speed of 10 m/s.

As shown in Figure 1, the MDTF consists of two vertical strut assemblies mounted on moveable carriages running along the measuring beams of the clearwater tank carriage. Each strut consists of an upper section (upper strut) and a lower section (lower strut). Attached to each upper section are two sets of linear bearings (upper and lower). Rails attached to the lower struts permit each lower strut to be retracted up and down relative to its corresponding upper strut. The upper portions of both forward and aft struts are mounted on carriages. The forward strut is bolted to its carriage at three locations. The aft strut is bolted to a frame assembly that is mounted on pillow block ball bearings that allow the strut to pivot about the across tank axis. At the bottom of each lower strut is a yoke which connects to the sting, a thick-walled tube (pipe) of varying outside diameter. The yokes permit the sting to rotate freely about the vertical axis and about a horizontal axis perpendicular to the sting.

Model loads are measured using a dynamometer (6 component balance) consisting of load cells and flexible links, as shown in Figure 1. Linear accelerometers and rate gyros are also installed. The dynamometer assembly is connected to the sting inside the model by means of a bolted flange arrangement.

Operational Issues

When operated under certain conditions, a number of problems can arise. Two examples are presented below.

Steady yaw angle test

In this case, because of the flexibility of the system (primarily due to the sting), steady hydrodynamic loading causes elastic deflections of the model which can increase or decrease the nominal yaw angle by several degrees. Furthermore, because of the relatively large mass of the model, the system has a low natural frequency and unsteady forces on the model can cause vibrations, which further contaminate the measurements.

Harmonic yaw test

Depending on the ratio of input frequency to natural frequency and damping in the system, the output motion of the model can be amplified from the nominal value. If resonance is approached, significant elastic deflections can occur, causing additional loading on the MDTF structure and associated components (dynamometer, bearings, drive motors, yoke connections, etc.).

Objectives

One objective of this project was to carry out a structural and dynamic (vibration) analysis of the model/sting/MDTF system in order to obtain the following information.

- Natural frequencies and mode shapes
- Static deflections, force and moment reactions and stresses
- Dynamic effects due to vibration

The other objective was to identify techniques for correcting measured test data to take into account the flexibility of the system.

Natural Frequency and Linear Static Loading Analysis

In order to carry out the necessary calculations, the following data were required.

- Mass properties of model
- Dynamometer stiffnesses
- Structural data for MDTF
- Previous test runs for the Albert model for calculating damping ratio in free vibration

The natural frequency and linear static load analyses were carried out using the ALGOR finite element (FE) program.

Reference Axes

The tank axes are defined so that its x axis is along the length of the tank, positive towards the beach, its z axis is positive upward, and the y axis is across the tank. In the subsequent analysis, it was more convenient to use reference axes attached to the model. In this case, the origin of the reference xyz coordinate system is located at the balance resolving centre (BRC) of the dynamometer. It is also assumed that the BRC has the same location as the centre of buoyancy of the prototype (scaled down). The xyz body fixed axes make angles with respect to the tank axes for nonzero roll, pitch or yaw. The x axis lies along the longitudinal axis of the model and sting, positive towards the tail. Assuming the roll angle is zero, the y axis is horizontal (port to starboard), perpendicular to the sting and the z axis lies in the vertical plane, perpendicular to the sting, positive upward. In the case of zero roll, pitch and yaw, these axes coincide with the tank axes. Note that the body fixed axes x and z used in this report are opposite in sense to those shown in Figure 2.

Mass Properties of Albert Model

The Albert submarine model consists of an outer shell and an inner structure which allows for connection to the dynamometer, which is connected to the forward end of the sting. When submerged, part of the interior of model becomes flooded with water. To make the model as neutrally buoyant as possible, part of the model is filled with foam.

The weight of the Albert model (including dynamometer and other components inside the model) in air, and the apparent weight in water were provided (measured values).

The in-air mass was 584 kg and the in-water apparent weight was 3450 N.

For dynamic calculations, the total masses and mass moments of inertia with respect to the xyz axes were based on the following contributions

- model in air
- floodwater inside submerged model
- added hydrodynamic masses and mass moment of inertia

  The in-air and floodwater masses, moments of inertia and centre of mass locations were provided by IOT or calculated based on data provided.

The added mass properties for the Albert prototype were provided by DRDC. The values were then scaled down, based on the model having a scale of 1:15. The length of the Albert model (non-truncated) was 4.683 metres. The length of the actual model (truncated) was slightly less.

In order to determine the in-air and floodwater mass moments of inertia relative to the xyz axes, the locations of the in-air and floodwater centres of mass relative to the BRC were also calculated.

For all model installations, the sting segment aft of the coupling (located forward of the forward strut) was 7-inch pipe with a wall thickness of 0.5 inches. The short pipe segment connected to the aft yoke was 6-inch OD (0.5 inch wall).

The sting extension for the Albert model is a steel pipe having a 6 inch outside diameter and 1/2 inch wall thickness. In this case, the distance from the BRC to the coupling connecting the extension to the 7-inch OD pipe is 2.951 metres.

The mass properties of the model are summarized as follows.

Mass Properties of Albert Model				
	In air	Floodwater	Added	Total
m_x (kg)	584.0	366.6	30.4	981.0
m_y (kg)	584.0	366.6	1106.4	2057.0
m_z (kg)	584.0	366.6	763.9	1714.5
I_x (kg-m^2)	19.9	10.7	25.7	56.3
I_y (kg-m^2)	421.8	170.2	867.4	1459.4
I_z (kg-m^2)	412.5	170.0	1167.0	1749.5

Mass Properties of Other Models

The mass properties of the Albert model were used to estimate the corresponding values for two other hypothetical models, 2.8 metre and 6 metre lengths (non-truncated). The values were obtained by an appropriate scaling of the Albert values, and are presented as follows.

Mass Properties of Other Models		
Total	2.8 m. model	6.0 m. model
m_x (kg)	209.7	2063.3
m_y (kg)	439.7	4326.2
m_z (kg)	366.5	3605.8
I_x (kg-m^2)	4.3	194.3
I_y (kg-m^2)	115.5	5038.8
I_z (kg-m^2)	133.7	6040.0

The sting extension for the 2.8 metre model is assumed to be a steel pipe having a 3.5 inch outside diameter and 3/8 inch wall thickness. In this case, the distance from the BRC to the coupling connecting the extension to the 7-inch OD pipe is assumed to be 1.764 metres which was obtained by scaling down the corresponding value for the Albert model.

The sting extension for the 6 metre model is assumed to be a steel pipe having an 8 inch outside diameter and 3/4 inch wall thickness. In this case, the distance from the BRC to the coupling connecting the extension to the 7-inch OD pipe was 3.781 metres.

Dynamometer Stiffnesses

The translational and rotational stiffnesses of a dynamometer used in previous tests were provided (in English units) by IOT and converted to SI units. Rotational stiffnesses were then converted from N-m/degree to N-m/radian. In order to assess the importance of the dynamometer flexibility on the overall behaviour of the model/MDTF system, natural frequencies for each of the six degrees of freedom were calculated based on the simple formula

$$f_n = \frac{1}{2\pi}\sqrt{k/m}$$

where f_n is natural frequency in cycles per second (hz), k is translational stiffness (N/m) or rotational stiffness (N-m/rad) and m is model mass (kg) or mass moment of inertia (kg-m^2), depending on the context. Basically the dynamometer model is treated as six independent one degree of freedom systems, which is not strictly correct because the dynamometer vibrations in the six degrees of freedom would in fact be coupled. The present approach is used only to provide approximate estimates so that the frequencies can be compared with values for the entire system as shown later in this report.

The stiffnesses, mass properties and natural frequencies are given as follows, where Dof is a degree of freedom (xyz translation or rotation).

Dynamometer Stiffnesses and Natural Frequencies			
Dof	k (N/m, N-m/rad)	m (kg, kg-m^2)	f_n (hz)
x trans	1.17×10^7	981	17.4
y trans	4.38×10^6	2057	7.3
z trans	3.50×10^6	1714	7.2
x rot	4.16×10^5	56	13.7
y rot	1.61×10^6	1459	5.3
z rot	3.80×10^6	1750	7.4

Structural Data

The main structural components considered in the analysis were the following.

- various OD sting extensions (steel)
- 6-inch OD sting segment (steel)
- 7-inch OD sting segment (steel)
- lower strut (aluminum)
- upper strut (aluminum)

Material Properties

Generic values of mass density ρ, elastic modulus E and Poisson's ratio ν were used for the two materials, as follows.

Material Properties			
	ρ (kg/m^3)	E (GPa)	ν
Steel	8000	200	0.29
Aluminum	2700	73	0.33

Sectional Properties

For the purpose of specifying sectional properties in the ALGOR finite element analysis it was necessary to specify local axes for the beam elements comprising the sting and struts. First, recall that the xyz axes are attached to the model/sting which can rotate in the horizontal and vertical plane. The sting local 1 direction lies along the x axis. In this case the local 2 direction is selected to be along the y axis, and the local 3 direction along the z axis. For each strut, the local axis 1 is along the strut longitudinal axis, the local 2 direction in the across tank direction. In the case of zero yaw angle, the strut local 2 direction coincides with the y axis. For non-zero yaw angles the strut local 2 direction makes an angle in the horizontal plane with the y axis.

The struts were thin-walled hollow members. For the various models, the sting extensions had different lengths and cross-sectional dimensions.

The cross-sectional area A, moments of inertia (2nd moments of area) I_2 and I_3, torsion constant J and section moduli S_2 and S_3 are listed below.

Sectional Properties				
	7-in OD pipe (1/2-in wall)	6-in OD pipe (1/2-in wall)	3.50-in OD pipe (3/8-in wall)	8-in OD pipe (3/4-in wall)
A (m^2)	6.60×10^{-3}	5.56×10^{-3}	2.375×10^{-3}	1.102×10^{-2}
I_2 (m^4)	2.27×10^{-5}	1.36×10^{-5}	1.898×10^{-6}	4.722×10^{-5}
I_3 (m^4)	2.27×10^{-5}	1.36×10^{-5}	1.898×10^{-6}	4.722×10^{-5}
J (m^4)	4.53×10^{-5}	2.72×10^{-5}	3.795×10^{-6}	9.443×10^{-5}
S_2 (m^3)	2.55×10^{-4}	1.79×10^{-4}	4.269×10^{-5}	4.647×10^{-4}
S_3 (m^3)	2.55×10^{-4}	1.79×10^{-4}	4.269×10^{-5}	4.647×10^{-4}

	Upper strut	Lower strut
A (m^2)	1.49×10^{-2}	2.88×10^{-2}
I_2 (m^4)	7.54×10^{-4}	3.79×10^{-4}
I_3 (m^4)	2.58×10^{-4}	1.50×10^{-4}
J (m^4)	5.67×10^{-4}	3.21×10^{-4}
S_2 (m^3)	2.52×10^{-3}	2.06×10^{-3}
S_3 (m^3)	1.41×10^{-3}	1.47×10^{-3}

Additional Mass Properties of Sting and Struts for Dynamic Analysis

The interior of the sting is flooded with water. Therefore, for dynamic analysis the additional vibrating mass per unit length of the floodwater was calculated by multiplying the interior sting area (based on the inside diameter) by the density of water ρ_w (1000 kg/m^3). Also the hydrodynamic added mass per unit length of the sting was estimated by assuming that it was equal to the sting exterior area (based on OD) multiplied by ρ_w. An equivalent mass density ρ_{eff}, taking into account the material mass (density ρ_s = 8000 kg/m^3), floodwater mass and added mass, was calculated using the following formula.

$$\rho_{\text{eff}} = \frac{(\rho_s A_m + \rho_w A_i + \rho_w A_o)}{A_m}$$

where $A_m = \pi\left(D_o^2 - D_i^2\right)/4$ is the material cross-sectional area, $A_i = \pi D_i^2/4$ is the inside cross-sectional area and $A_o = \pi D_o^2/4$ is the exterior cross-sectional area of the sting segment. The effective mass densities for the various sting outside diameters are presented in the following table.

Sting OD (in)	Effective density (kg/m^3)
7.0	14546
6.0	13530
3.5	12227
8.0	12885

This approach implies that the additional effect of the floodwater and added mass is effective equally in all three axis directions. However, in reality, the effect in the longitudinal (x) direction would be much less.

Initially, the effect of portions of the lower struts immersed in water was taken into account. In the worst case, both struts were immersed approximately 2.8 m. Methods for calculating the effective flooded mass and added mass for the struts are complicated by the fact that the struts pierce the free surface. Therefore, as an approximation, the additional mass was simply calculated by multiplying the approximate enclosed area (0.0688 m^2 based on the outside cross-sectional dimensions) of the strut section by 2.8 m and then multiplying by the density of water. This value was then multiplied by a factor of 2 to take into account both the floodwater and added mass. The resulting value of 385 kg was then used for a lumped mass at each of the yoke locations. This additional mass is probably much higher than the actual value. When incorporated into the FE model, it was found that it had virtually no effect on the values of the lowest two natural frequencies. Therefore, it was decided to neglect this additional mass, in view of the uncertainty in its actual value.

Finite Element Analysis

Natural frequency and linear static load FE analysis was carried out using ALGOR. The sting and struts were modelled with 3D beam elements having the material and sectional properties presented earlier in this report. For the dynamic analysis, the model was considered as a lumped mass having the properties presented earlier.

Various assumptions and simplifications were made. Figure 3 shows relevant dimensions and locations for the case involving the Albert model, where both lower struts are fully extended. (Drawings of geometries for other configurations are not presented in this report).

- The forward end of the sting was assumed to be located at the BRC of the model (pt. a).
- The sting extension was located between a and b. (This distance changed for the different models).

- The 7-inch OD sting segments extended from b to d and the short 6-inch OD segment from d to f.
- The lower struts (cg and ei) extended to the centre-line of the sting.
- At each connection between a strut and the sting (c or e), end releases were incorporated to take into account the presence of the yoke. For each lower strut this corresponded to specifying rotational end releases about the y axis and z axis for the strut element node at the connection. For the case of non-zero yaw angle, the y axis does not coincide with the local 2 direction for the strut. Since it was necessary to have the release axis coincide with the local axis of the strut element, the orientation of the beam element adjacent to the yoke position was changed to coincide with the y axis. For this element the corresponding moments of inertia are incorrect, but since the element was short in length, the effect was small. Another option would have been to replace the bottom element of each strut with one having the properties of a solid circular cross-section (representing the contribution of the yoke), in which case the local 2 axis can act in any horizontal direction.
- For simplicity, each strut assembly is assumed to consist of a lower strut which is connected to the corresponding upper strut (gh or ij) at the elevation of the upper linear bearing mounted on the upper strut. It was assumed that each lower strut tended to bend relative to the upper strut at this location. The ball screw assembly, effect of linear bearings between lower strut and upper strut, the tubular frame supports, etc. were not modelled in detail. Each ball screw, which is driven by a motor at the top of its respective upper strut and lowers or raises the lower strut has minimal bending stiffness compared to the lower strut. On the other hand, the ball screw would normally provide a small amount of axial stiffness in addition to that of the lower strut. The lower strut is free to slide up and down inside the upper strut. Therefore, axial load is not transferred directly from the lower strut to the upper strut at the linear bearing locations, although the ball screw does produce an axial force reaction at the top of the upper strut.
- Each upper strut is rigidly supported at an elevation approximately half-way between the carriage location and the top of the strut (h and j). In reality, each upper strut is supported by means of a three-dimensional tubular frame arrangement.

This particular FE idealization is reasonable for the purpose of obtaining natural frequencies, static deflections of the model, reactions, and very approximate estimates of stresses in the struts. However, for a detailed stress analysis (to check for structural failure) a much more detailed FE idealization would be required, in order to check loading not only on the structural components but also on bearings, welded connections, motor drives, ball screws, etc.

Natural Frequencies and Mode Shapes

The lowest six natural frequencies and corresponding mode shapes of the Albert model were determined for the case of zero yaw and pitch angle angles, where both lower

struts were fully extended, as shown in the following table. Figure 4 shows the mode shapes for Modes 1 and 2.

Natural Frequencies (hz) of Albert Model						
Mode No.	1	2	3	4	5	6
Frequency	0.66	1.46	3.41	4.34	5.44	7.55

The following table shows the two lowest natural frequencies (Mode 1-"yaw" and Mode 2 -"pitch") for various strut positions, pitch angles and yaw angles for the Albert model, a 2.8 metre model and a 6.0 metre model. Natural frequencies corresponding to modes 3 to 6 were also calculated for the 2.8 metre model and the 6.0 metre model but are not presented here.

Natural Frequencies (hz) for Modes 1 and 2						
Configuration	Albert model		2.8 m. model		6.0 m. model	
	Yaw	Pitch	Yaw	Pitch	Yaw	Pitch
pitch +30°, forward strut fully retracted	1.02	1.45	2.32	3.07	0.65	0.99
pitch +30°, forward strut at mid-stroke	0.84	1.45	1.98	3.05	0.52	0.98
pitch -30°, forward strut at mid-stroke	0.83	1.46	2.01	3.07	0.52	0.99
pitch -30°, forward strut fully extended	0.68	1.45	1.67	3.06	0.42	0.99
both struts fully extended	0.66	1.46	1.64	3.08	0.41	0.99
both struts fully retracted	1.00	1.46	2.33	3.08	0.64	0.99
both struts at mid-stroke	0.82	1.46	1.98	3.08	0.51	0.99
yaw 30°, struts fully extended	0.73	1.46	1.79	3.08	0.45	0.99
yaw 30°, struts at mid-stroke	0.89	1.46	2.12	3.08	0.55	0.99
yaw 30°, struts fully retracted	1.06	1.46	2.47	3.09	0.68	0.99

Note that because of symmetry a yaw angle of $-30°$ gives the same results as for a yaw angle of $+30°$.

In Mode 1 the vibration takes place in the horizontal plane and is characterized by bending of the sting and, simultaneously, oscillation in the y direction of the bottoms of the lower struts where, at a given instant, the direction of motion of one strut is opposite to the other . This could be characterized as a "yaw mode". Mode 2 takes place in the vertical plane and consists of bending of the sting relative to the bottom end of the forward strut. In this mode, the axial stiffness of the struts precludes any significant deformation of the portion of the sting between the two struts. This mode is, for convenience, called a "pitch mode".

Note that the two lowest frequencies are much lower than the dynamometer/model natural frequencies, which implies that the dynamometer flexibility, if it had been incorporated in the FE idealization would have a secondary effect on the natural frequencies. On the other hand, the forward end of the sting is assumed to be located at the BRC. This assumption would tend to overestimate the bending flexibility.

Previous tests with the Albert model yielded natural frequencies for the yaw and pitch modes in the case of zero yaw angle and both struts fully extended, the natural frequencies being 0.65 hz and 1.36 hz for yaw and pitch, respectively. The values obtained from the FE analysis, 0.66 hz and 1.46 hz, respectively, are in good agreement, considering the simplified FE idealization.

Linear Static Load Analysis

A linear static load analysis was carried out for the Albert model for the case of zero yaw and both struts fully extended (worst case scenario). Seven load cases were considered.

The first six load cases consisted of applying forces and couples to the model (BRC location), namely unit forces (1 kN= 1000 N) in each of the x, y, z directions and unit couples (1 kN-m= 1000 N-m) about the x, y, z axes.

The weight of the model, sting and struts was taken into account in load case no. 7. In this case, the apparent weight of the Albert model in water (3450 N) was applied as a force in the negative z direction. The weights of the sting and struts were automatically taken into account by ALGOR by specifying a gravity load multiplier -1 in the z direction and incorporating a load case multiplier of 1 for gravity. The buoyancy force on the sting was neglected. Furthermore, the weights of the additional components inside the struts were not taken into account. This load case tends to provide an overestimate because of the fact that each upper strut, in reality, is not directly connected to its corresponding lower strut.

The results of the seven load cases could then be used in future to determine deflections, internal forces and moments and stresses for any loading scenario, using appropriate linear combinations.

In this particular configuration, for the struts, the local directions $1, 2, 3$ correspond to the z, y, x directions, respectively. For each of the seven load cases, the following quantities were recorded.

- Model deflection dx, dy, dz in x, y, z directions, respectively
- Axial force (F_z), shear forces (F_y and F_x) and bending moment (M_x) in each strut at its connection with the sting. At the yoke connections, the struts do not resist torque (about z axis) or bending about the y axis. Therefore, M_z and M_y are zero at the yoke location for all cases.
- For each strut, maximum axial stress (σ_a) and maximum bending stresses (σ_{by} = stress caused by bending about y-axis and σ_{bx} = stress caused by bending about x-axis) in each strut. Note that these results are very approximate because of the simplified strut idealization.

Transverse shear stresses in the struts were neglected. (The sectional geometry and length of the struts is such that this is a reasonable assumption).

Shear forces (N), axial force (N) and bending moment (N-m) on each strut at its yoke location are shown as follows.

Shear Forces, Axial Force and Bending Moment on Strut at Yoke Location									
		Forward Strut				Aft Strut			
Load Case		F_x	F_y	F_z	M_x	F_x	F_y	F_z	M_x
1	x force-1 kN	−500	0	0	0	−500	0	0	0
2	y force-1 kN	0	2692	0	2956	0	−1692	0	−2956
3	z force-1 kN	0	0	2692	0	0	0	−1692	0
4	x couple-1 kN-m	0	0	0	−713	0	0	0	−287
5	y couple-1 kN-m	0	0	500	0	0	0	-500	0
6	z couple-1 kN-m	0	−500	0	−675	0	500	0	675
7	Weight	0	0	−12680	0	0	0	6380	0

The maximum axial and bending stresses (MPa) for the struts are given in the following table.

Maximum Axial and Bending Stresses							
		Forward Strut			Aft Strut		
Load Case		σ_a	σ_{bx}	σ_{by}	σ_a	σ_{bx}	σ_{by}
1	x force-1 kN	0	0	1.065	0	0	1.064
2	y force-1 kN	0	8.143	0	0	4.338	0
3	z force-1 kN	0.1806	0	0	0.114	0	0
4	x couple-1 kN-m	0	0.506	0	0	0.2032	0
5	y couple-1 kN-m	0.034	0	0	0.034	0	0
6	z couple-1 kN-m	0	1.424	0	0	1.424	0
7	Weight	1.059	0	0	0.2208	0	0

Because of the geometry of the system (lies in xz plane), many of the deflection components are zero for the various load cases. The non-zero deflection components of the model BRC are as follows, for each load case.

Model BRC Deflections		
Load Case		Deflection (m)
1	x force-1 kN	$dx = +5.65 \times 10^{-4}$
2	y force-1 kN	$dy = +2.51 \times 10^{-2}$
3	z force-1 kN	$dz = +5.83 \times 10^{-3}$
4	x couple-1 kN-m	$dy = +1.37 \times 10^{-3}$
5	y couple-1 kN-m	$dz = +2.41 \times 10^{-3}$
6	z couple-1 kN-m	$dy = -6.45 \times 10^{-3}$
7	Weight	$dz = -2.35 \times 10^{-2}$

The values in the preceding tables can be used for actual load cases by appropriate combining and scaling using linear superposition.

Dynamic Response

Effect of Damping

Small Amplitude Damping

In general, the model dynamics are non-linear because the hydrodynamic forces are non-linear functions of the degrees of freedom. For small vibration displacements, the system could be approximated as a linear system. In this case, the standard mass-spring-viscous damper analysis can be used. The damping ratio is a parameter required to predict the vibration response of the system. Measurements of acceleration versus time (due to free vibration) were obtained from previous tests. The standard logarithmic decrement method for successive amplitudes of a decaying sinusoid was used. The logarithmic decrement δ is given by

$$\delta = \ln \frac{X_n}{X_{n+1}}$$

where X_n is the peak amplitude in cycle n. The damping ratio ζ was calculated using the formula

$$\zeta = \frac{\delta}{2\pi}$$

which is valid for small values of ζ.

Yaw Test In this test, the model had been undergoing a steady yaw angle test, and the system was allowed to vibrate freely after the carriage had stopped. The vibrations were small amplitude. The acceleration record for the yaw test was a well-defined decaying sinusoid.. Using the first five peaks, four successive X_n/X_{n+1} ratios were calculated (theoretically, the values should be the same) and averaged, yielding a value of 1.159, and a logarithmic decrement of $\delta = 0.147$. The resulting damping ratio was $\zeta = 0.023$. Some of the damping is attributed to structural damping and part to hydrodynamic damping.

Pitch Test For the pitch test, the acceleration record was not a pure decaying sinusoid. The decaying signal contained at least two frequency components (modulated signal). Therefore, applying the logarithmic decrement method was not considered accurate. However, to check the order of magnitude of the decay in the signal, a value of ζ was estimated from the first two peaks, yielding a value of 0.039.

Magnification Factor

In certain types of model tests (harmonic yaw, pitch, sway or heave, for example) the model is nominally subjected to a time varying motion related to the input motion of the struts on the MDTF. Because of the flexibility of the system these motions or magnified by vibrations. This is particularly important if the model test involves a harmonic excitation near resonance. Although the system is a multi-degree of freedom system, an estimate of the effect of the flexibility system on amplifying or magnifying

the motion can be carried out using the magnification factor concept used for a one degree of freedom mass, spring, damper system. In this case the magnification factor (MF) is given by

$$MF = \frac{1}{\sqrt{(1-r^2)^2 + (2\zeta r)^2}}$$

where $r = f/f_n$ (excitation frequency/natural frequency) is the frequency ratio and ζ is the damping ratio of the system. For excitation frequencies much lower than the natural frequency, the MF is close to unity, whereas at resonance MF is higher. Ideally, MF should be as close to unity as possible. If not, there is an amplification of the input acceleration.

Large Amplitude Damping

The previous estimate of damping ratio is not realistic for large amplitude motions. (For small vibrations, the damping force is assumed to be proportional to velocity). However, in harmonic sway or yaw tests with large amplitudes of motion (0.1 to 0.5 metres) the hydrodynamic forces which are non-linear functions of velocity produce a non-linear amplitude dependent damping.

Therefore, for large amplitudes of vibration, the damping ratio of 0.023 would tend to be much too low, and would overestimate the magnification effect. Therefore, the damping ratio obtained from the small amplitude free vibration tests would be inappropriate and was not used in subsequent dynamic analysis. Instead, an estimate of dynamic response was obtained using a mathematical model of the system which included the non-linear hydrodynamic loads and flexibility of the system.

Estimates of Loading in Harmonic Sway Test

In order to provide an estimate of dynamic loading on the MDTF during a harmonic sway test, a simple mathematical model was developed to take into account the flexibility of the system, the hydrodynamic loading on the model and the inertial loading caused by the acceleration of the model in the sway direction.

The hydrodynamic side force on the model (not including added mass effect which is taken into account separately) is given in the form

$$Y = \frac{\rho}{2} L^2 \left(Y'_v u v + Y'_{v|v|} v \, |v| \right)$$

where Y'_v and $Y'_{v|v|}$ are hydrodynamic coefficients. L is the model length, ρ is the density of water, u is the model velocity in the x direction and v is the model velocity in the y direction (with respect to body axes).

The differential equation of motion for the model is

$$m\ddot{y} + b_1\dot{y} + b_2\dot{y}\,|\dot{y}| + ky = ky_b$$

where

$$b_1 = -\frac{\rho}{2} L^2 Y'_v u \quad b_2 = -\frac{\rho}{2} L^2 Y'_{v|v|}$$

m is the total mass of the model (including added mass and floodwater mass), k is the stiffness of the system, $y_b(t)$ is the input displacement (motion of strut carriages) and $y(t)$ is the displacement of the model at the BRC location in the sway direction. The model velocity component in the y direction is $v = \dot{y}$.

The model is restrained so that its body axis x is always aligned with the longitudinal tank axis. Therefore, the velocity component u is the towing carriage speed, assumed to be constant.

For a harmonic test, $y_b(t) = A\cos\omega t$, where ω is the excitation frequency in rad/s and A is the input displacement amplitude (of the strut carriages). Dividing the equation by m and using the relationship $k/m = \omega_n^2$, where ω_n is the natural frequency of the system in rad/s, yields the following non-linear differential equation.

$$\ddot{y} + c_1\dot{y} + c_2\dot{y}\,|\dot{y}| + \omega_n^2 y = \omega_n^2 A\cos\omega t$$

where $c_1 = b_1/m$ and $c_2 = b_2/m$. The initial conditions are assumed to be $y(0) = 0$ and $\dot{y}(0) = 0$. (Only steady state conditions associated with the external excitation are of interest so that the initial conditions are selected arbitrarily).

The force transmitted from the model to the MDTF (force measured by dynamometer) is

$$F = k(y - y_b)$$

The drag force is

$$Y = -b_1\dot{y} - b_2\dot{y}\,|\dot{y}|$$

and the acceleration of the model ($a = \ddot{y}$) is

$$a = (Y - F)/m$$

The non-linear differential equation of motion was solved numerically for output displacement $y(t)$ and velocity $\dot{y}(t)$ using MATLAB. Time records of y, a, and F were then plotted for a time span after transients had decayed and steady state conditions were in effect. The maximum values (amplitudes) of these quantities were also determined and recorded. For a particular vehicle model, the analysis was carried out for different values of input displacement A (metres), input frequency $f = \omega/(2\pi)$ and towing speed u.

The magnification factor (MF) of displacement for a particular input amplitude A and excitation frequency f is defined to be the ratio of output amplitude divided by the input amplitude, for steady state conditions. Therefore,

$$MF = y_{\max}/A$$

where $y_{\max}$ is the steady-state amplitude of $y(t)$.

The previous analysis refers to the case where the flexibility of the system (sting, MDTF struts) is taken into account (*flexible* case). If the system was *rigid*, then the model motion would be identical to the strut motion. In this case, the model displacement is $y_R(t) = A\sin\omega t$, and the measured force can be calculated from the expression

$$F_R = Y_R - ma_R$$

where Y_R and a_R are calculated using the strut acceleration and velocity.

Example: Albert Model

For the Albert model, the total mass is $m = 2057$ kg in sway and the natural frequency is $f_n = 0.66$ hz (for the case where both struts are fully extended). The stiffness of the system is $k = m\omega_n^2 = m\,(2\pi f_n)^2 = 3.537 \times 10^4$ N/m. The coefficients $Y_v' = -0.055$ and $Y_{v|v|}' = -0.15$ were provided by DRDC. Plots are presented in Figures 5 to 10 for various cases. Note the following.

- As an example of the type of output that the numerical simulation can generate, Figures 5 and 6 plot sway displacement, sway acceleration and measured force for an input amplitude of 0.4 m, input frequency of 0.25 hz and two towing speeds, 0 m/s (for reference purposes) and 4 m/s.

- Figures 7 and 8 plot magnification ratio (MF) versus input frequency for different amplitudes and towing speeds. The magnification ratio applies to the sway displacement and acceleration. Note that for a given frequency and towing speed, the value of MF decreases with amplitude and, for a given frequency and amplitude, the value of MF decreases with towing speed. This behaviour is due to the effect of the non-linear hydrodynamic force acting on the model. The peak value of MF occurs at a frequency which is slightly less than the natural frequency.

- Figures 9 and 10 show plots of measured force amplitude (maximum force) $F_{\max}$ versus amplitude for different input frequencies, input amplitudes and towing speeds. In all cases $F_{\max}$ increases with increasing input amplitude. For a given towing speed, and input amplitude, $F_{\max}$ increases as the input frequency increases. The dashed curves in the plots are for the hypothetical case where the system is perfectly rigid and the model follows the strut motion. The difference in the rigid and flexible cases is quite significant in most cases.

A linear static analysis was carried out to determine the loading on the lower struts due to a force F in the y direction applied at the model BRC location. This analysis used a different FE idealization than the one described earlier in this report. In this case the upper struts were removed and it was assumed that the lower struts were simply supported at the lower and upper linear bearing locations. The forward strut is the most heavily loaded for this type of loading.

For the Albert model case, with both struts fully extended, it was found that the quantity of interest could be expressed as a numerical factor C multiplied by the measured force F, where F is in kN. The numerical factors for each quantity of interest are presented in the following table.

Quantity (Forward Lower Strut)	**Units**	C
Force F_y on strut at yoke location	kN	2.692
Moment M_x on strut at yoke location	kN-m	1.219
Force F_y on lower linear bearing	kN	8.224
Moment M_x on strut at lower bearing	kN-m	4.918
Maximum bending stress on lower strut	MPa	3.346

Using the predicted values of F from the harmonic sway dynamic response analysis, bearing loads and bending stresses were plotted for various ranges of towing speeds, input frequencies and input amplitudes. Examples of these calculations are shown in the plots in Figures 11 to 14. Additional data for the various quantities is presented in the spreadsheet printout in Figures 15 and 16. This spreadsheet and an interactive computer program (MATLAB m-file) was supplied to IOT.

Note that, as mentioned previously, this data applies to the Albert model with both struts fully extended. For other strut extensions, the natural frequency and stiffness of the system would change, with corresponding changes to the quantities plotted.

Example: DREA-DSUB Model

The length of the DSUB model was $L = 4.013$ m. Hydrodynamic coefficients $Y'_v = -0.027834$, $Y'_{v|v|} = -0.072$ and $Y'_{\dot{v}} = -0.016186$ (added mass coefficient) were provided by DRDC. The added mass in sway was

$$\frac{\rho}{2}L^3 Y'_{\dot{v}} = 523 \text{ kg}$$

The model mass in air was 348.6 kg and the floodwater mass was 367.3 kg. Therefore, the total mass was $m = 1239$ kg (substantially less than the 2057 kg mass of the Albert model). It is assumed that the BRC of the DSUB model is located at approximately the same distance from the forward yoke as the Albert model. Therefore, the system stiffness for the case where both struts are fully extended is approximately the same as for the Albert model configuration, namely, $k = 3.537 \times 10^4$ N/m. In this case, the lowest natural frequency f_n of the DSUB model can be estimated based on the fact that f_n is inversely proportional to the square root of mass. Therefore, for the DSUB model

$$f_{n,\text{DSUB}} = f_{n,\text{ALBERT}}\sqrt{\frac{m_{\text{ALBERT}}}{m_{\text{DSUB}}}} = 0.66\sqrt{\frac{2057}{1239}} = 0.85 \text{ hz}$$

In this case, test results are available for harmonic sway. Data from four runs for sway acceleration and sway force for various combinations of input amplitude and frequency are plotted in Figures 17 to 20 along with predicted results obtained from the numerical simulation described previously. In the last two runs (Figures 19 and 20), the strut motions did not follow the command signal so that the measured acceleration and force are not periodic with constant amplitude, unlike the first two runs (Figures 17 and 18). The predicted values of maximum acceleration and maximum force agree reasonably well with the test results, notwithstanding the fact that for the last two runs, there were problems with the tests. Consequently, this increases the level of confidence in using the numerical simulation for the dynamic response of the Albert model described earlier.

Steady Yaw Test Corrections

In a steady yaw test the hydrodynamic side force and yawing moment produce lateral and angular deflections of the model because of flexibility effects. The actual yaw angle

for the model is increased or decreased by the amount of angular deflection of the sting at the BRC location. In order to provide data on this effect a number of linear static FE analyses were carried out for the Albert model configuration. The parameters varied were strut extension and nominal yaw angle. Values of y deflection and angular deflection of the sting were obtained at the BRC location, forward yoke location and aft yoke location for two load cases (side force of F_y = 1000 N and yawing moment of M_z = 1000 N-m). The data is plotted in Figures 21 to 23. The data was also supplied to IOT in a spreadsheet, as shown in Figure 24.

Certain sign conventions are used, as follows.

- In top view the applied couple M_z is counter-clockwise.
- In top view, a positive yaw angle corresponds to a counterclockwise rotation of the model.
- A positive applied force F_y and corresponding y deflection are positive in the positive y direction. The corresponding angular deflection of the sting at the BRC location is negative.
- A positive applied couple M_z and corresponding angular deflection are positive (counter-clockwise). The corresponding y deflection of the sting at the BRC location is negative.

For example, if the yaw angle is positive, a positive F_y produces a positive y deflection, negative angular deflection at the BRC and subsequently decreases the yaw angle. Also, if the yaw angle is positive, a positive M_z produces a negative y deflection, positive angular deflection at the BRC and subsequently increases the yaw angle. The deflected shapes (top view) for the two load cases F_y and M_z are shown in Figure 25.

Note the following.

- The magnitudes of the deflections increase with strut extension.
- For a given strut extension, the magnitudes of the deflections decrease with yaw angle. This effect is attributed to the fact that the strut cross-sections are fixed in orientation so that as the yaw angle increases, the bending axis of a strut tends to rotate from its weak axis (along tank) towards the strong axis (across tank).

These calculations take into account the effect of a static load on the model in yaw. If unsteady forces are present, due to vortex shedding, for example, there would be additional deflections. These deflections would be oscillatory in nature.

In order to implement the correction scheme for arbitrary extensions and yaw angles, the data was polynomial fitted with respect to strut extension and yaw angle. The procedure involved calculating for each of the five yaw angles, a set of polynomial coefficients estimated using the deflection data for the range of extensions. Then, another set of polynomial coefficients was obtained by fitting the previously obtained coefficients with respect to the range of five yaw angles. This resulted in a polynomial coefficient matrix from which the deflection could be estimated for any extension and yaw angle. The program (MATLAB m-file) was submitted to IOT.

Therefore, in an actual test run, the results obtained can be used, by appropriate combining and scaling, to obtain the required deflections corresponding to the measured values of side force and yawing moment.

Conclusions and Recommendations

Natural Frequencies

The worst case scenario is where both struts are fully extended, for zero yaw angle. The lowest natural frequency of the system which corresponds to oscillation in the horizontal plane (yaw mode) may, for a particular model, have a value which is in or close to the range of frequencies used in harmonic sway or harmonic yaw tests.

Loading on MDTF

The internal loads and stresses can be estimated for the MDTF struts, assuming that the measured loading on the model is known. Depending on input frequency and amplitude, these loads and stresses can be significant in the case of a harmonic sway or yaw test because of the inertial forces generated by the acceleration and mass of the model. When the input frequency approaches the natural frequency, the input amplitude must be selected appropriately.

Dynamic Response (Harmonic Sway Test)

The system is non-linear because the hydrodynamic forces are non-linear functions of velocity. The dynamic response of the system (in a harmonic sway test, for example) depends on the model mass, stiffness of the system, towing speed, input amplitude, input frequency, and model hydrodynamic coefficients. In principle, the FE idealization and harmonic sway response analysis generated for this report could be used to predict the model motion, measured force and internal loads and stresses in the MDTF structure for a specified case.

The numerical simulation of harmonic sway presented in this report showed good agreement with test results for the DSUB model. Therefore, it should yield reasonable predictions of dynamic response for other models such as the Albert.

Correction Techniques

Steady Yaw Test

In the case of a steady yaw test, the results for sting deflections obtained in this report could be used with suitable combining and scaling to estimate the actual yaw angle for a particular set of side force and yaw moment by adding or subtracting the angular deflection at the model BRC to the nominal yaw angle, for a particular nominal yaw angle and strut extension.

Harmonic Sway Test

In the case of a harmonic sway test, the model motion is not exactly the same as the input, because of flexibility effects. Furthermore, although the input is simple harmonic, the measured model acceleration, although oscillatory, is not simple harmonic, because the system is non-linear. However, for cases where the output acceleration is approximately simple harmonic, the output sway displacement amplitude A_{out} can be estimated using the formula $A_{out} = a_{out}/(2\pi f)^2$ where a_{out} is the output (measured) acceleration of the model and f is the frequency in hz.

Based on test results for the DSUB model, there is apparently a problem with the struts not following the command signal for certain combinations of amplitude and frequency. However, since the trajectory of the model can be determined using acceleration measurements, the test results could in principle be used to obtain hydrodynamic data.

References

Fudge, G. & MacKay, M., (2003), *Marine Dynamic Test Facility - A Brief Development History*, LM-2003-01, Institute for Marine Dynamics, National Research Council of Canada

Williams C.D., Muselet, C., MacKay, M., Perron, C., (2002), *Physical Modelling of Vehicle Performance in High-Amplitude and High-Rate Manoeuvres*, presented at RTO SCI Symposium on "Challenges in Dynamics, System Identification, Control and Handling Qualities for Land, Air, Sea and Space Vehicles", held in Berlin, Germany 13-15 May 2002 and published in RTO-MTP-095

Figures

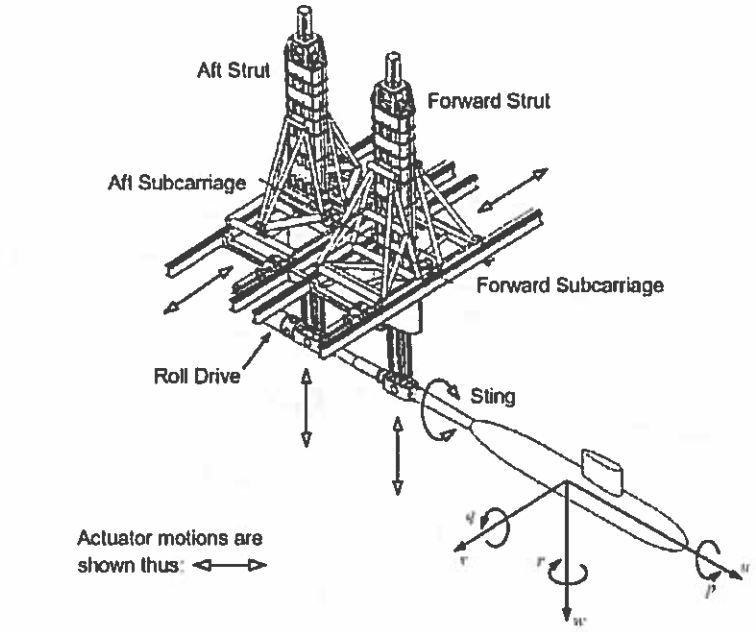

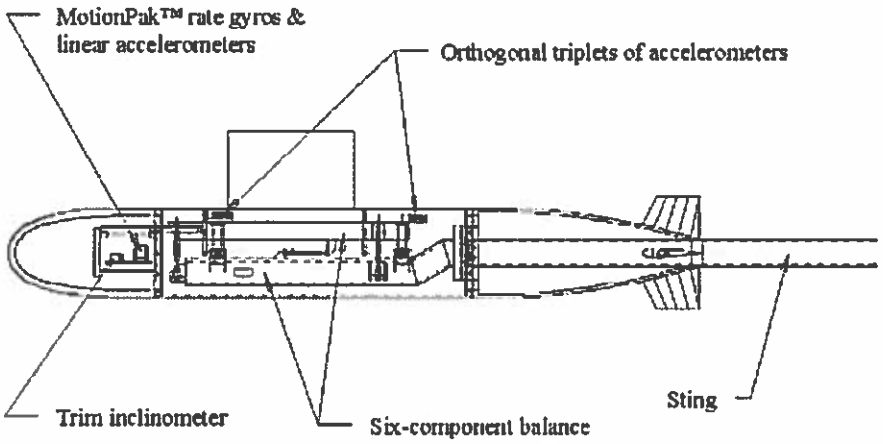

DREA Standard Submarine Model 4.5 m length, 0.5 m diameter

FIGURE 1: MDTF AND TYPICAL MODEL

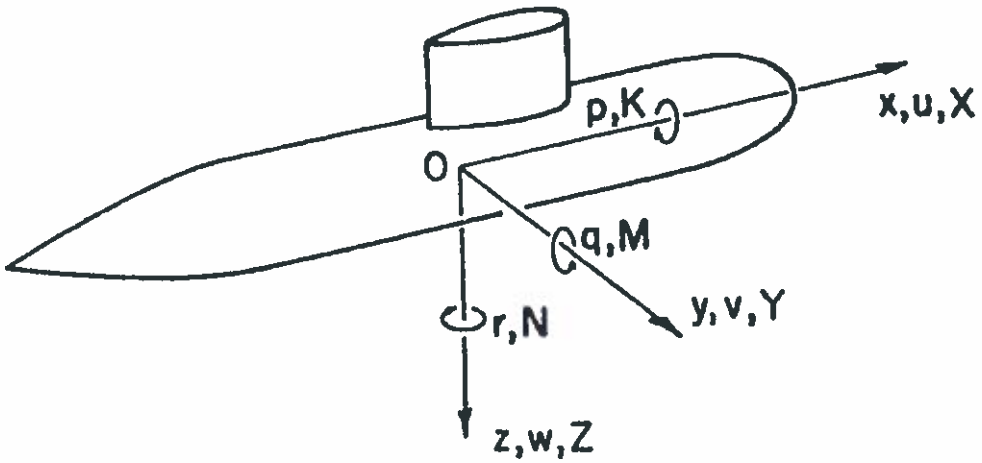

The body-fixed axes shown are used for hydrodynamic calculations. The reference x and z axes used in this report are opposite in sense to the ones shown above.

FIGURE 2: BODY-FIXED AXES

FE GEOMETRY FOR MODEL/STING/MDTF SYSTEM

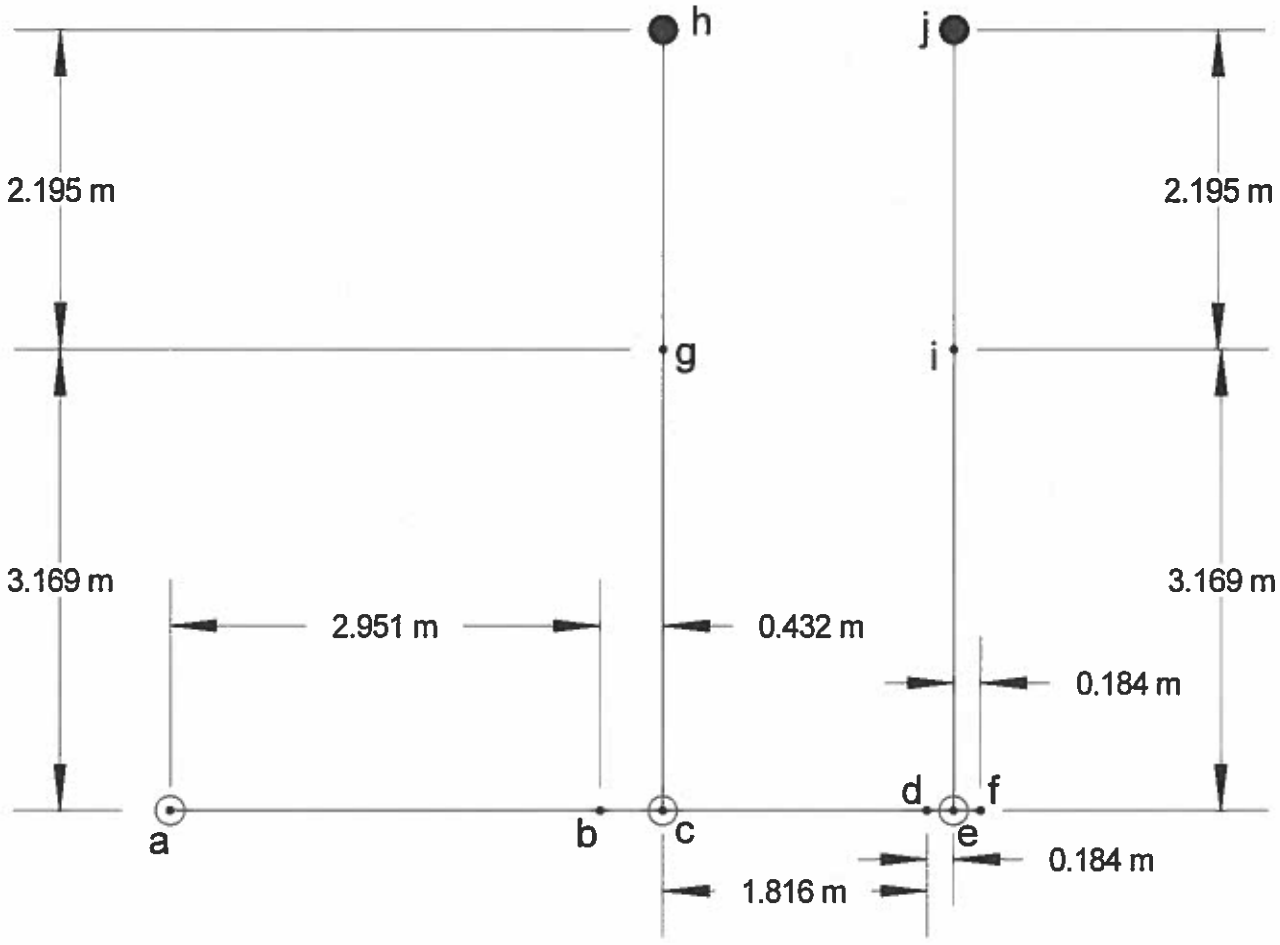

a: model BRC (origin of x,y,z coord system) - lumped mass
b: aft end of long segment of 6" OD sting
c: forward yoke - lumped mass for immersed portion of strut
d: aft end of 7" OD sting
e: aft yoke - lumped mass for immersed portion of strut
f: end of short segment of 6" OD sting
g: top of forward lower strut
h: top of forward upper strut: rigid boundary conditions
i: top of aft lower strut
j: top of aft upper strut: rigid boundary conditions

Note: +x to right, +y into page, +z up (origin at pt. a)

FIGURE 3
albert model: both struts fully extended

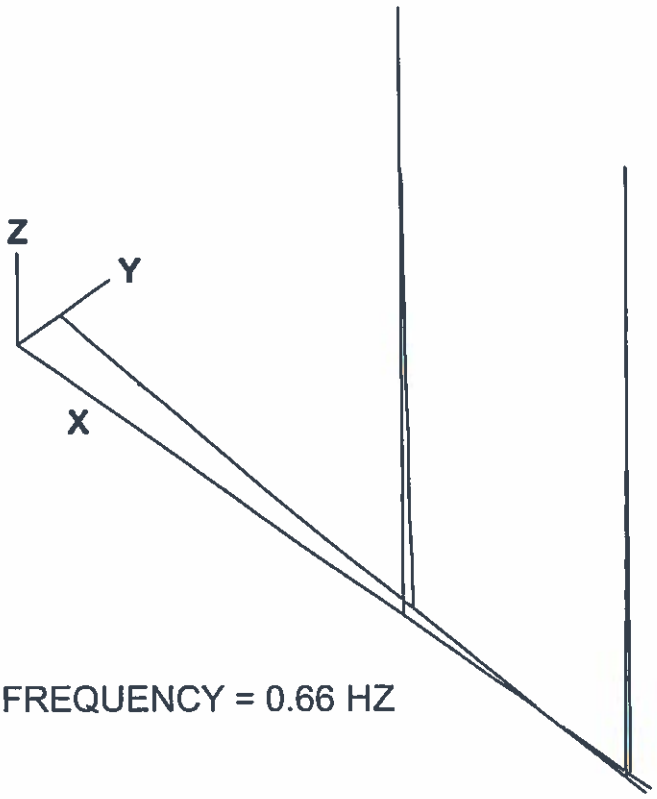

MODE 1: FREQUENCY = 0.66 HZ

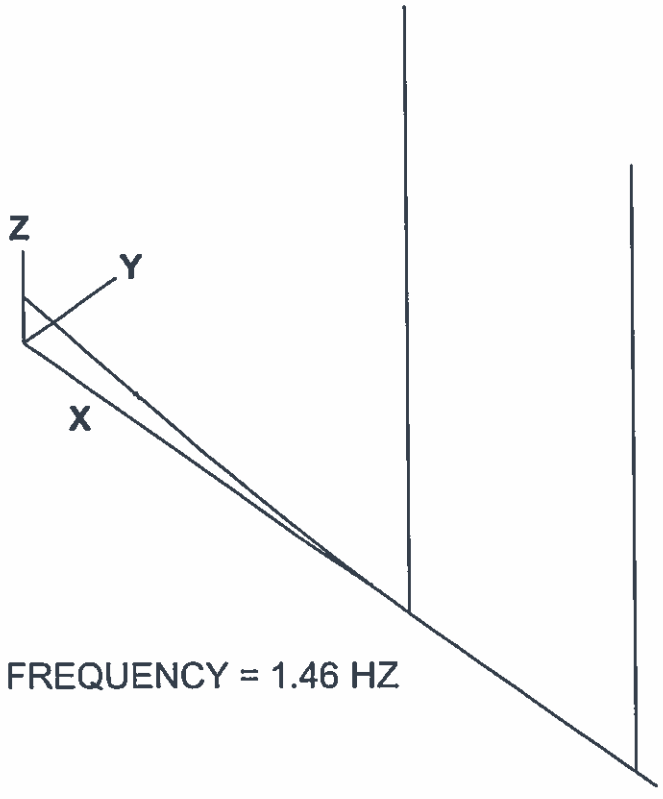

MODE 2: FREQUENCY = 1.46 HZ

FIGURE 4
mode shapes: albert model: both struts fully extended

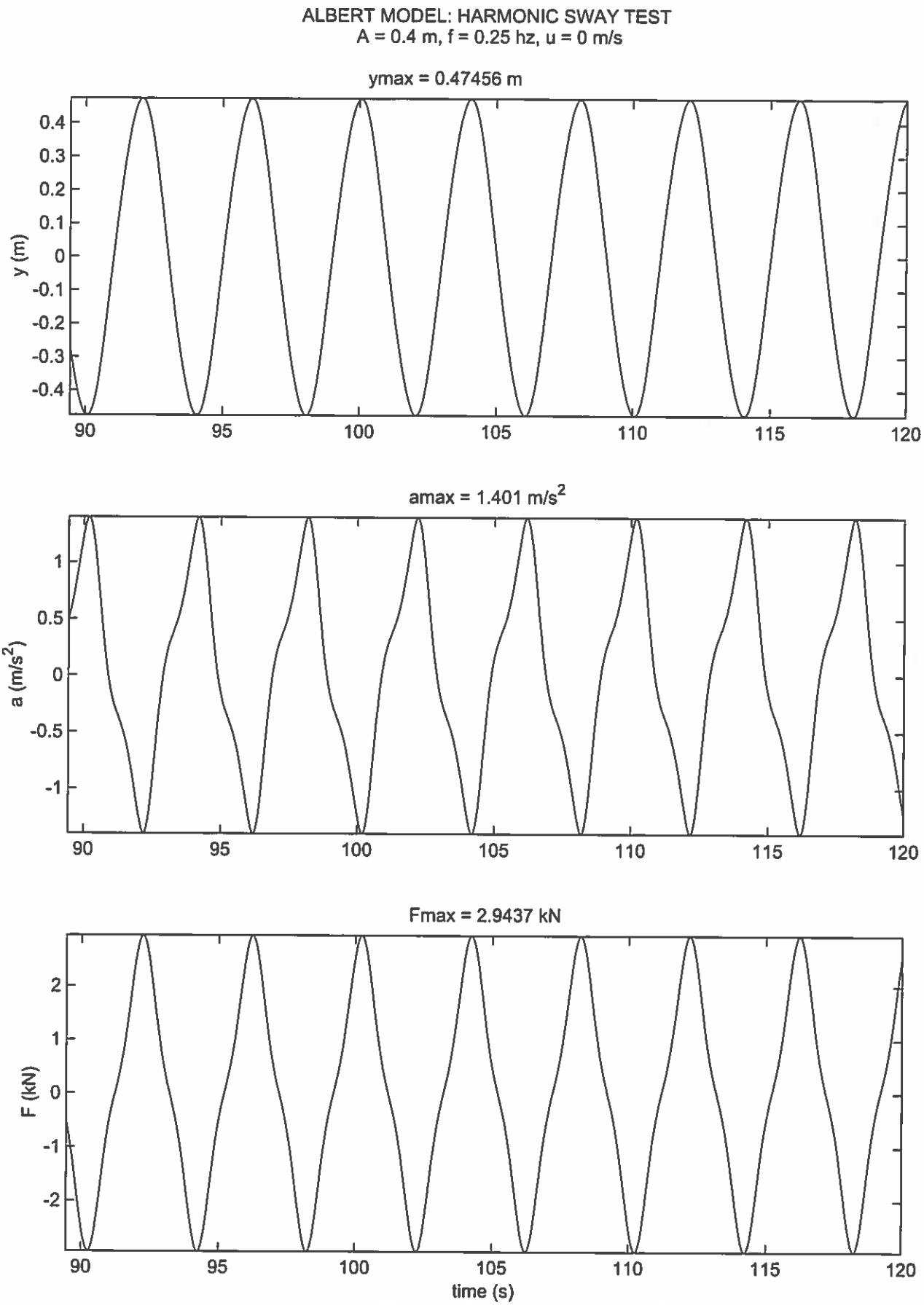

FIGURE 5
predicted sway response

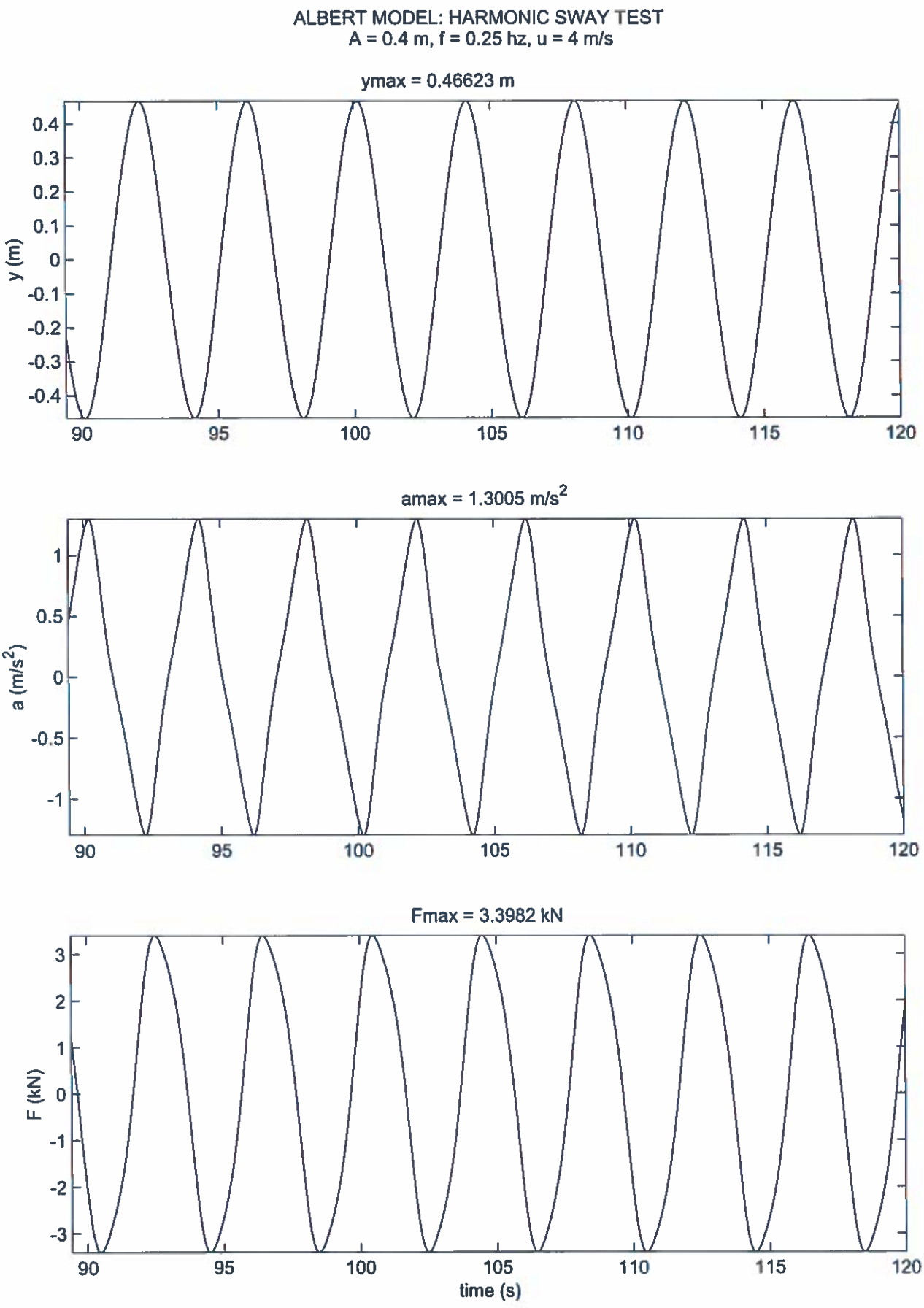

FIGURE 6
predicted sway response

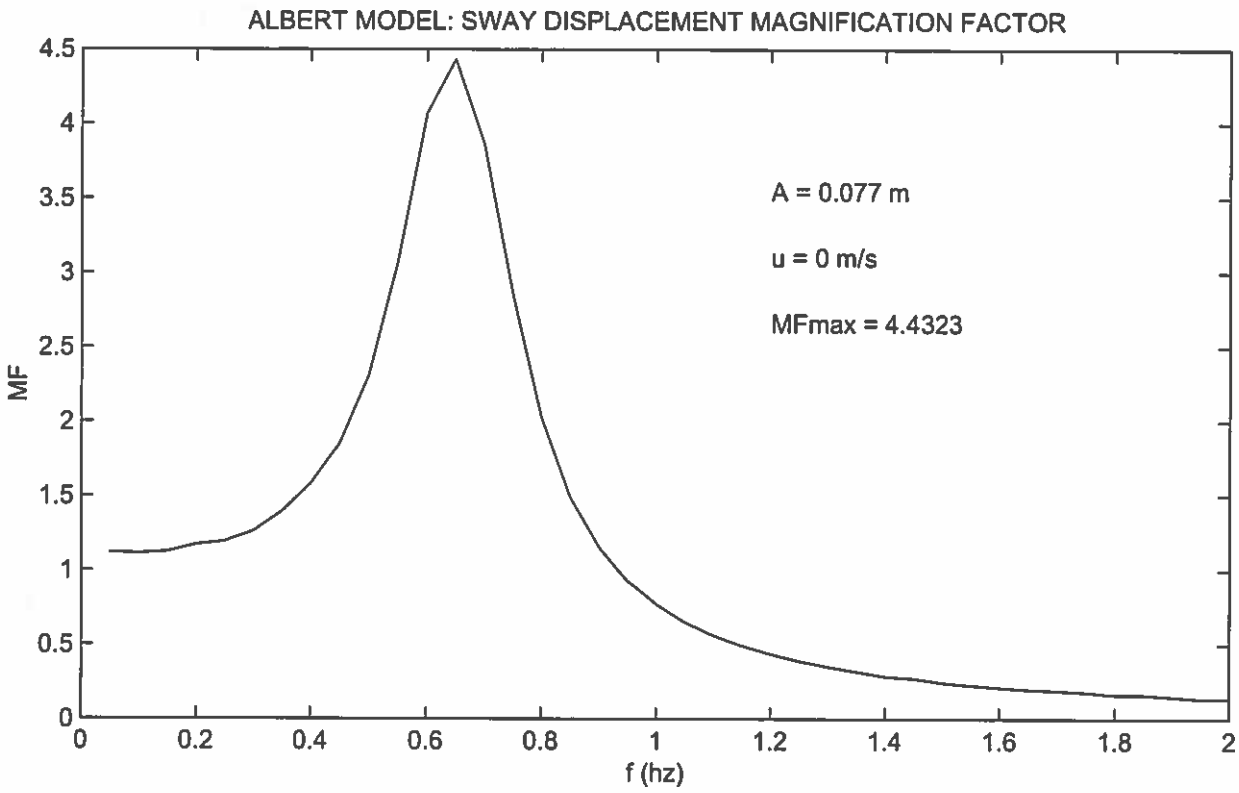

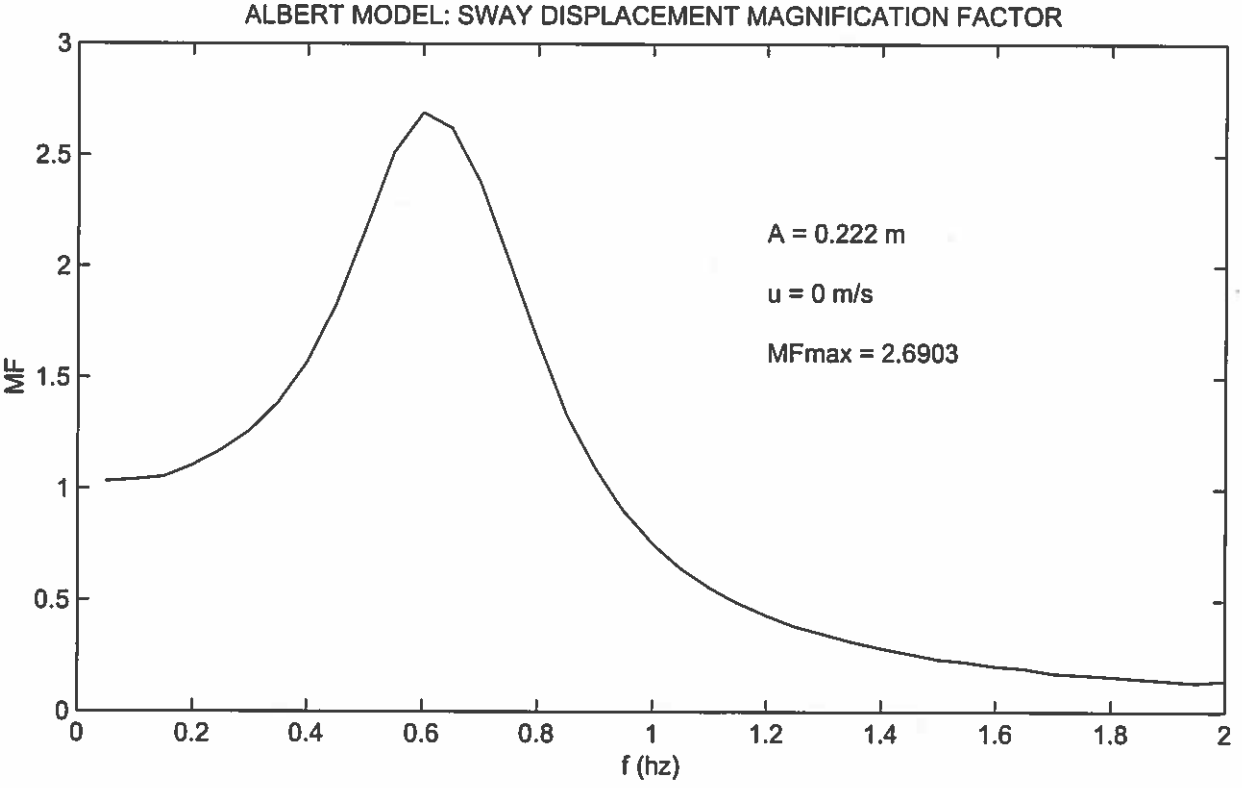

FIGURE 7
predicted sway response

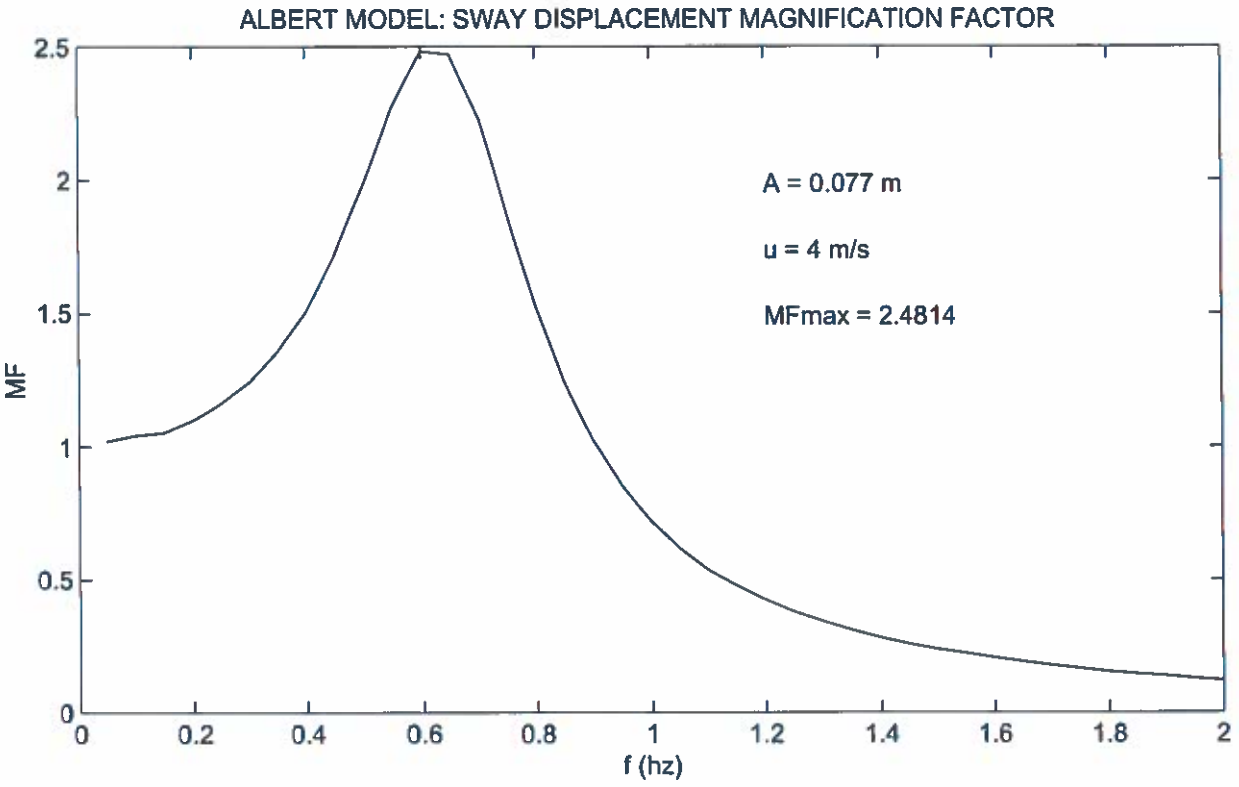

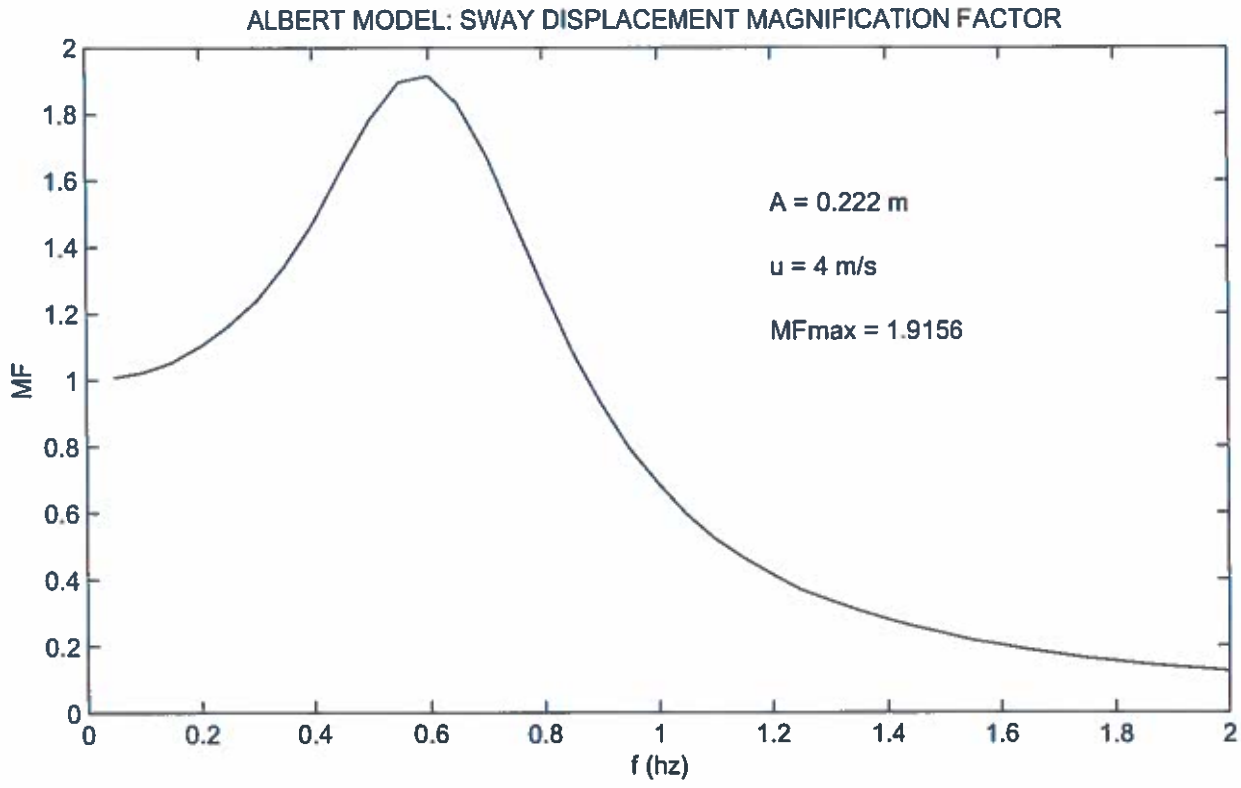

FIGURE 8
predicted sway response

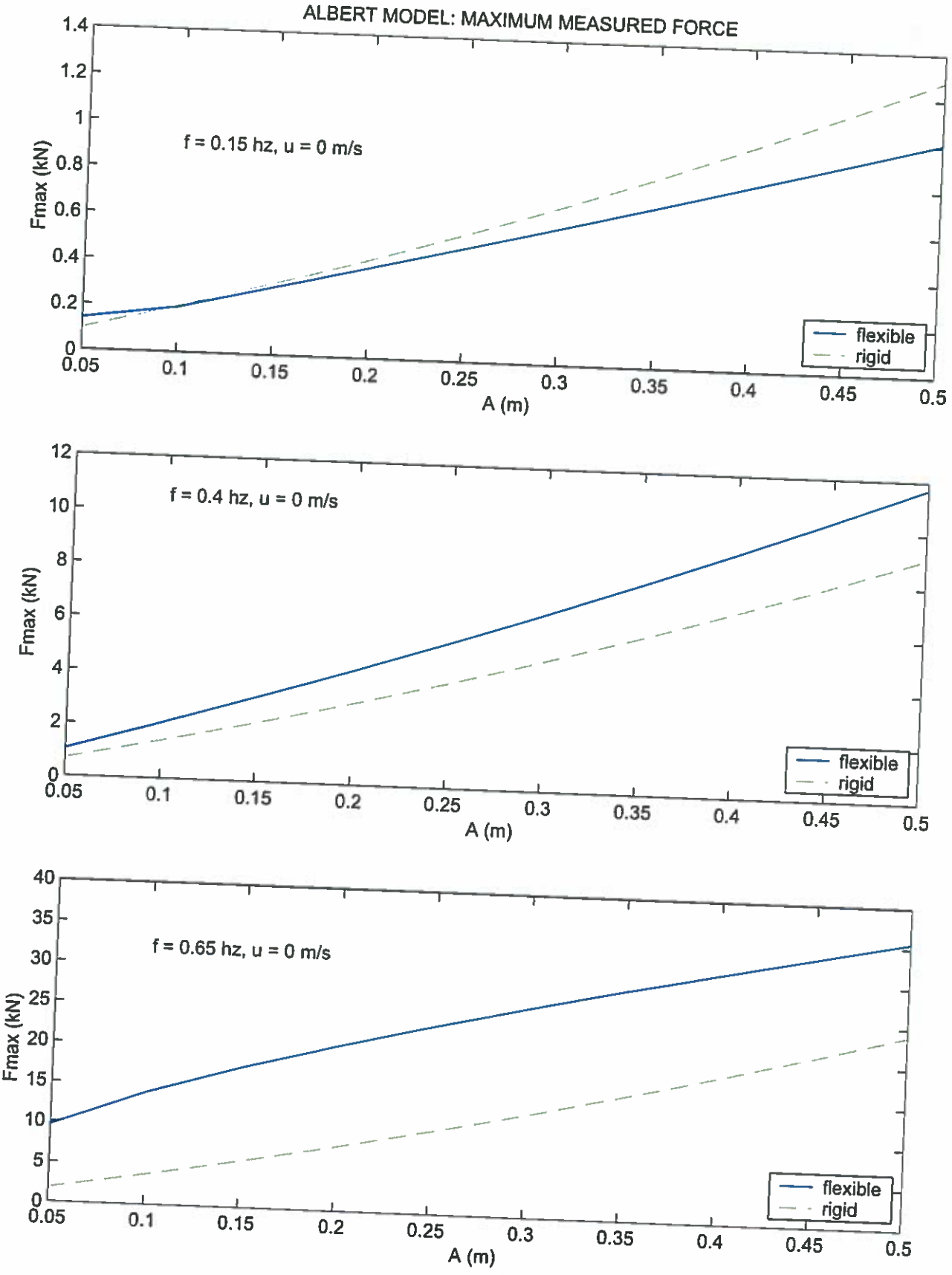

FIGURE 9
predicted sway response

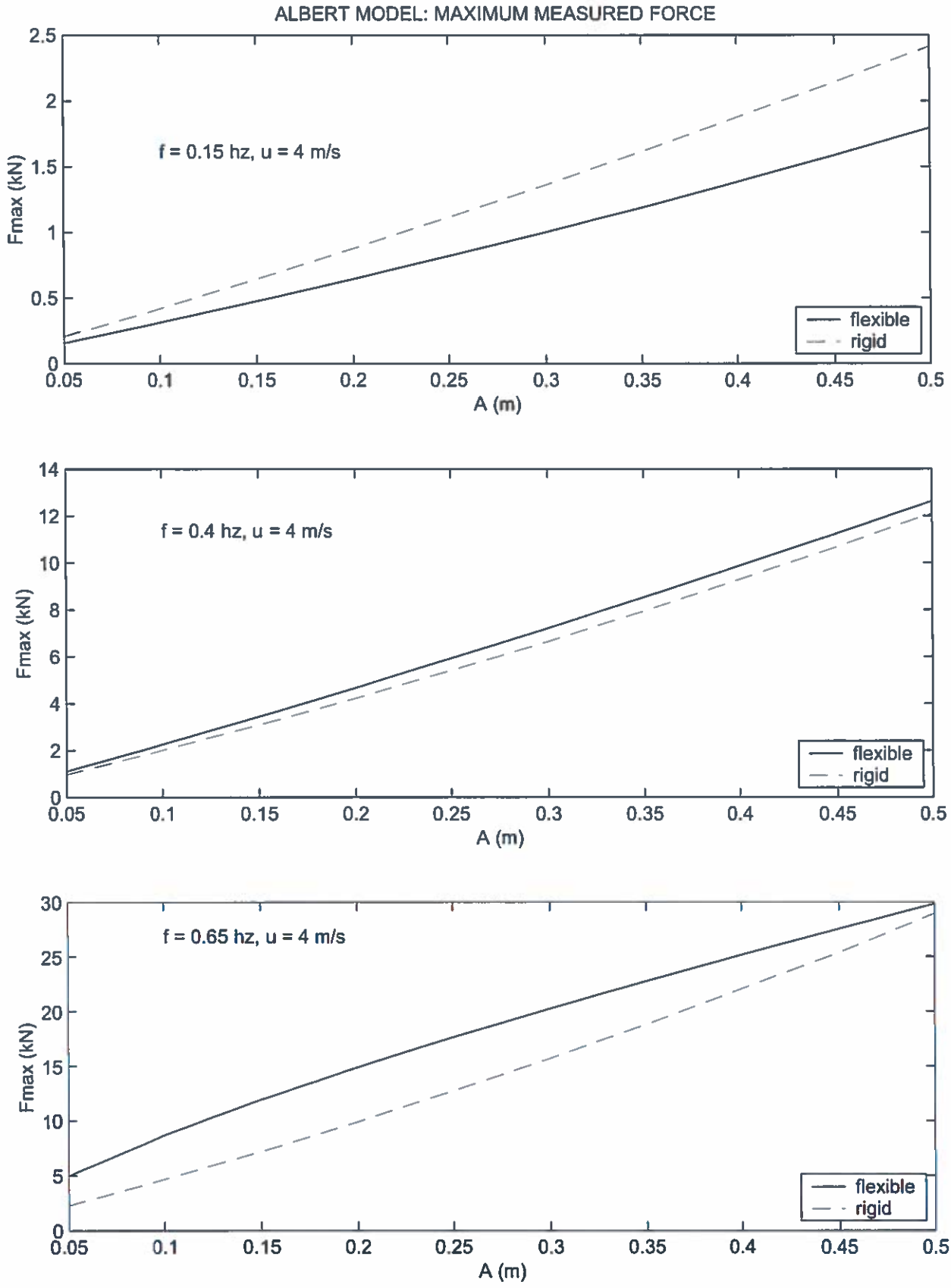

FIGURE 10
predicted sway response

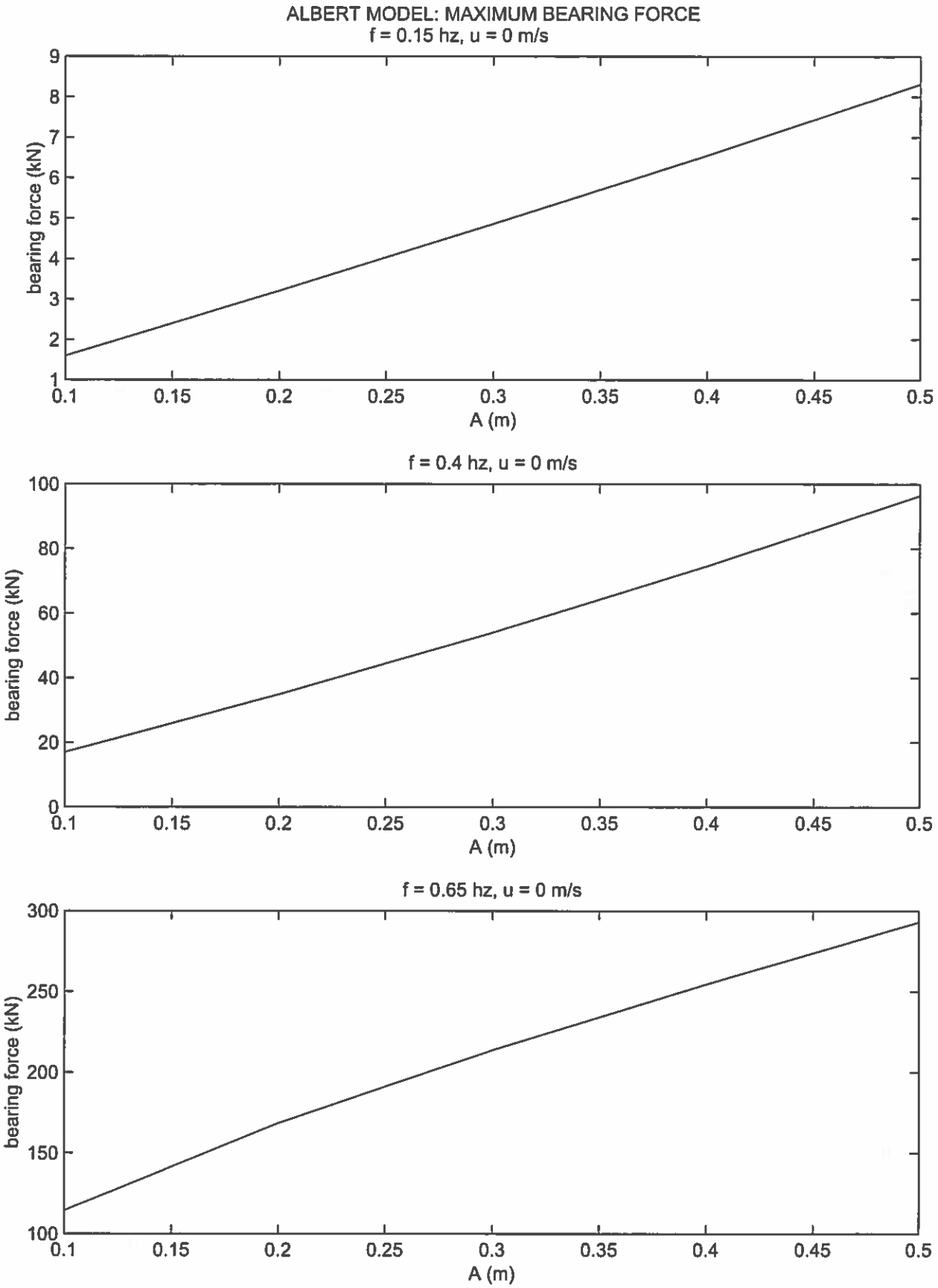

FIGURE 11
predicted sway response

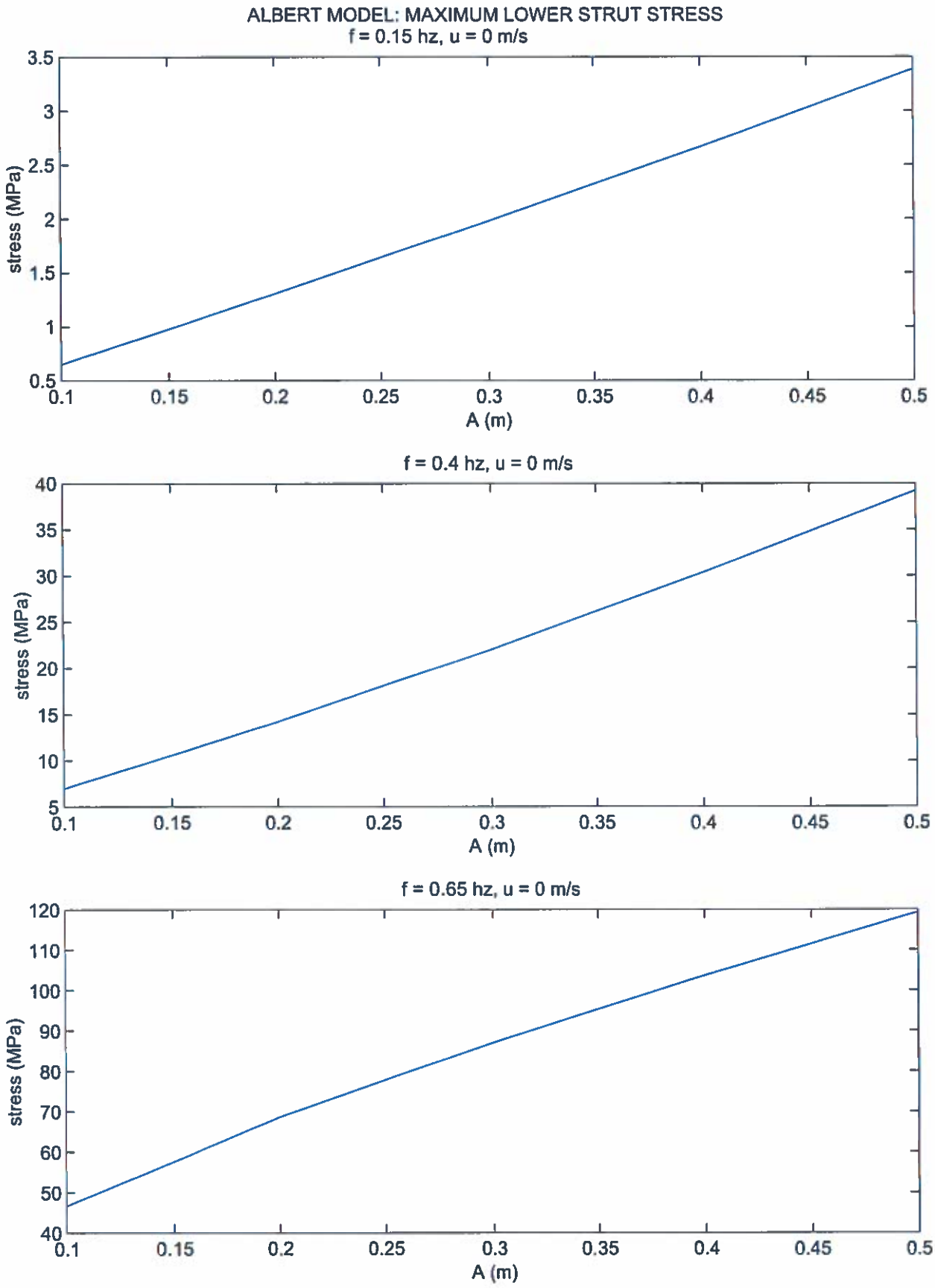

FIGURE 12
predicted sway response

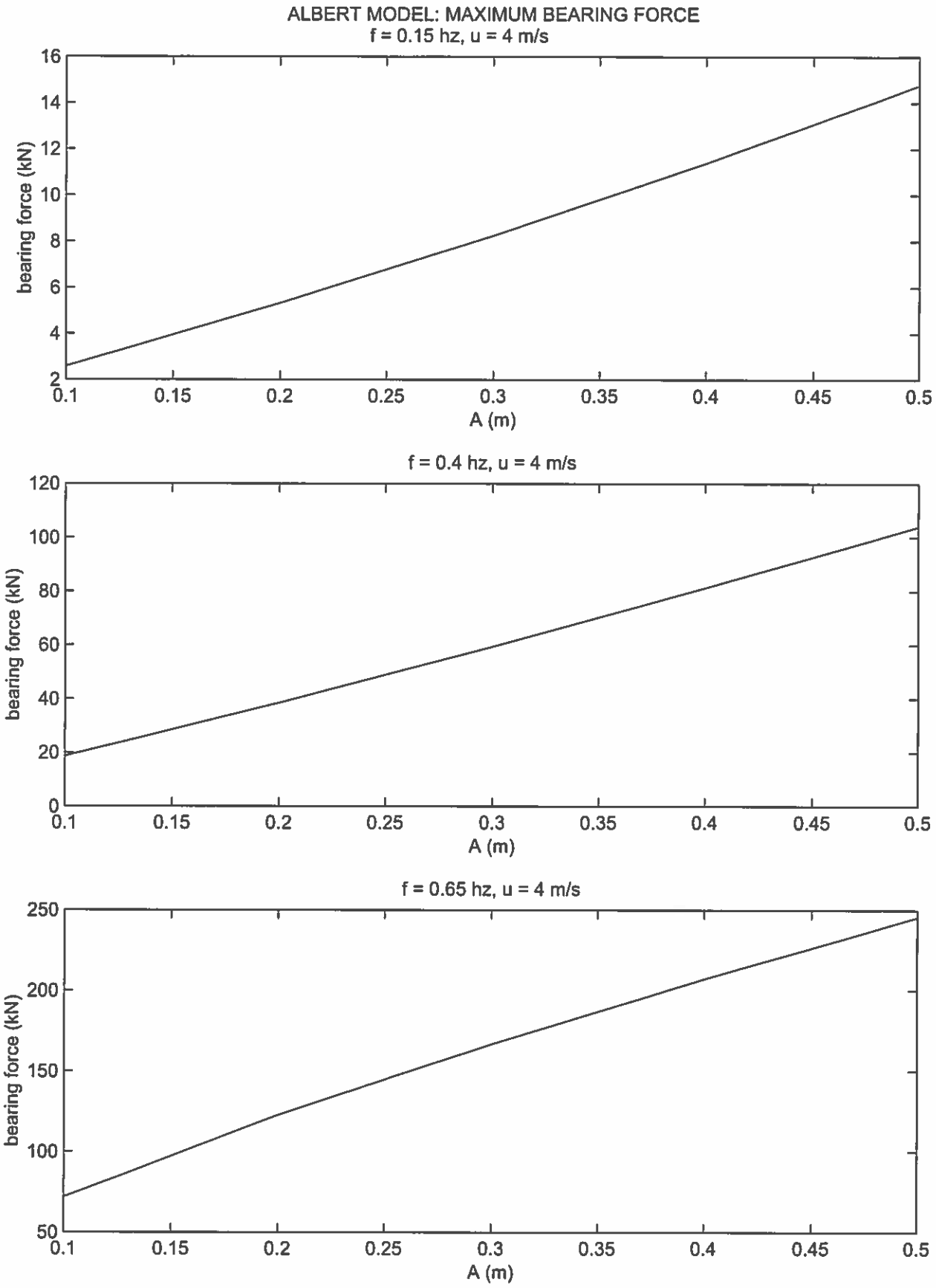

FIGURE 13
predicted sway response

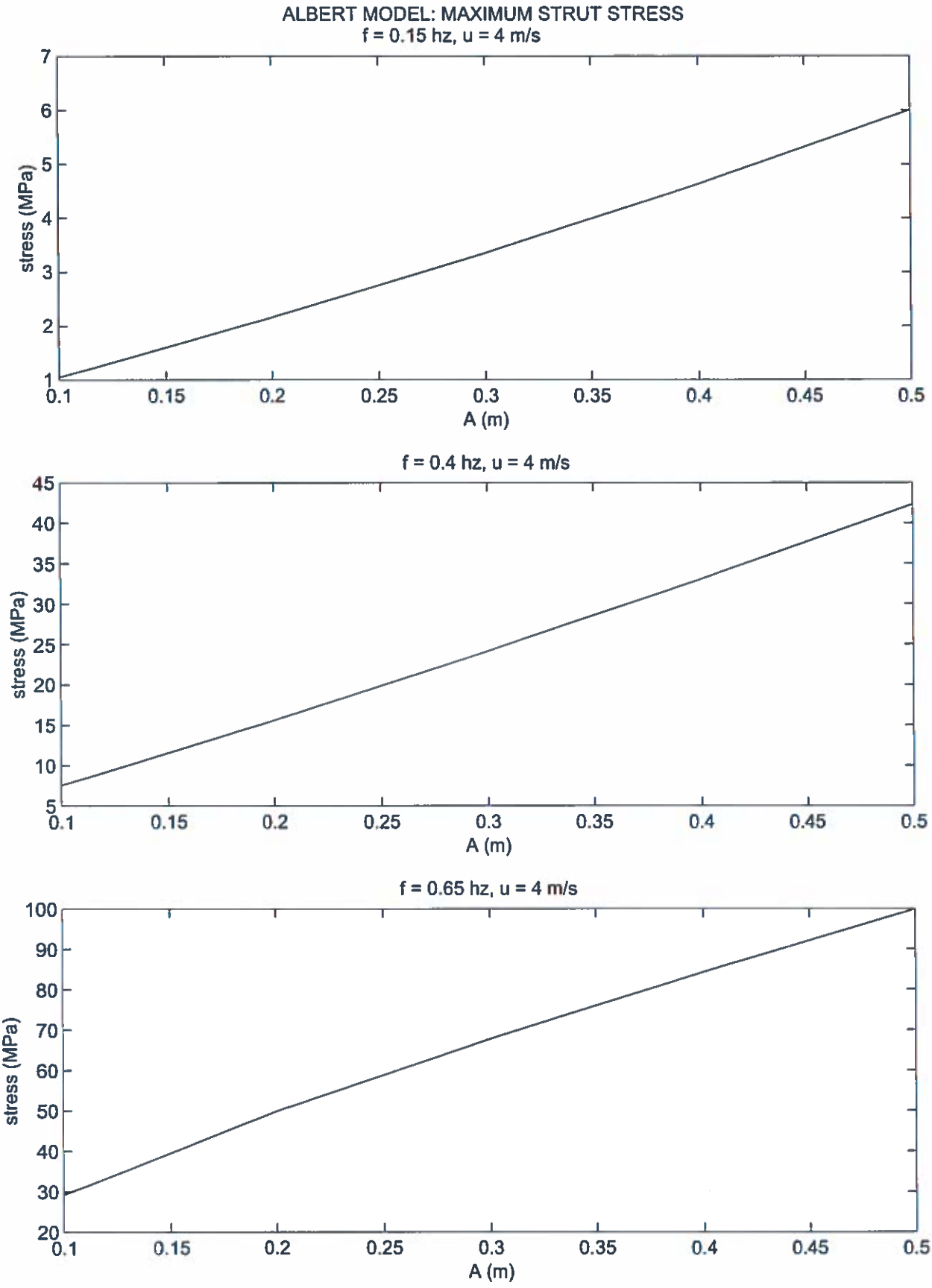

FIGURE 14
predicted sway response

HARMONIC SWAY TEST: ALBERT MODEL: BOTH STRUTS FULLY EXTENDED: PREDICTED LOADS ON MDTF: towing speed = 4 m/s

force fy measured by dynamometer (kN)

	ampl (m)													
f (hz)	0.05	0.10	0.15	0.20	0.25	0.30	0.35	0.40	0.45	0.50	0.55	0.60	0.65	0.70
0.10	0.089	0.181	0.276	0.373	0.474	0.577	0.683	0.792	0.904	1.019	1.137	1.258	1.381	1.508
0.15	0.155	0.314	0.477	0.646	0.821	1.002	1.189	1.384	1.585	1.794	2.009	2.232	2.462	2.699
0.20	0.244	0.490	0.737	0.988	1.242	1.500	1.763	2.031	2.308	2.600	2.905	3.223	3.555	3.898
0.25	0.375	0.766	1.172	1.593	2.026	2.472	2.929	3.398	3.877	4.369	4.869	5.380	5.902	6.432
0.30	0.548	1.121	1.717	2.339	2.981	3.649	4.333	5.036	5.764	6.507	7.267	8.045	8.838	9.649
0.35	0.784	1.600	2.449	3.330	4.241	5.182	6.152	7.148	8.167	9.214	10.287	11.374	12.487	13.613
0.40	1.112	2.261	3.448	4.669	5.927	7.217	8.535	9.880	11.248	12.637	14.045	15.477	16.906	18.380
0.45	1.577	3.182	4.811	6.464	8.135	9.820	11.521	13.227	14.934	16.666	18.396	20.114	21.847	23.582
0.50	2.245	4.444	6.603	8.720	10.809	12.838	14.893	16.929	18.899	20.827	22.818	24.780	26.715	28.536
0.55	3.157	6.030	8.696	11.220	13.636	15.955	18.242	20.455	22.625	24.760	26.855	28.931	30.926	32.932
0.60	4.217	7.634	10.655	13.434	16.049	18.548	20.905	23.287	25.558	27.796	29.962	32.126	34.234	36.313
0.65	4.984	8.735	11.968	14.905	17.652	20.256	22.768	25.183	27.544	29.837	32.074	34.316	36.478	38.576
0.70	5.123	9.047	12.433	15.502	18.364	21.042	23.625	25.994	28.589	30.962	33.269	35.555	37.751	39.947

force fy on forward lower strut at yoke location (kN)

	ampl (m)													
f (hz)	0.05	0.10	0.15	0.20	0.25	0.30	0.35	0.40	0.45	0.50	0.55	0.60	0.65	0.70
0.10	0.240	0.488	0.743	1.005	1.276	1.554	1.840	2.133	2.434	2.744	3.061	3.386	3.719	4.060
0.15	0.417	0.845	1.285	1.739	2.210	2.696	3.201	3.725	4.268	4.829	5.410	6.009	6.627	7.265
0.20	0.657	1.318	1.984	2.659	3.343	4.038	4.745	5.467	6.213	6.998	7.821	8.677	9.570	10.494
0.25	1.010	2.063	3.156	4.287	5.454	6.653	7.886	9.148	10.438	11.761	13.109	14.483	15.888	17.314
0.30	1.476	3.018	4.622	6.298	8.026	9.823	11.664	13.558	15.517	17.518	19.563	21.656	23.793	25.974
0.35	2.110	4.307	6.592	8.964	11.417	13.949	16.560	19.243	21.985	24.805	27.694	30.619	33.615	36.647
0.40	2.992	6.087	9.281	12.569	15.956	19.428	22.978	26.596	30.279	34.019	37.809	41.665	45.512	49.479
0.45	4.246	8.565	12.951	17.400	21.900	26.435	31.014	35.608	40.201	44.866	49.523	54.148	58.812	63.483
0.50	6.044	11.962	17.775	23.474	29.097	34.559	40.092	45.574	50.875	56.067	61.427	66.707	71.917	76.819
0.55	8.500	16.233	23.410	30.203	36.708	42.952	49.107	55.064	60.907	66.654	72.292	77.883	83.253	88.654
0.60	11.352	20.551	28.683	36.165	43.203	49.932	56.277	62.687	68.803	74.826	80.656	86.484	92.158	97.754
0.65	13.418	23.515	32.219	40.123	47.520	54.528	61.292	67.791	74.148	80.321	86.344	92.379	98.198	103.845
0.70	13.791	24.354	33.470	41.732	49.435	56.645	63.599	69.975	76.961	83.350	89.559	95.714	101.627	107.537

bending moment mx on forward lower strut at yoke location (kN-m)

	ampl (m)													
f (hz)	0.05	0.10	0.15	0.20	0.25	0.30	0.35	0.40	0.45	0.50	0.55	0.60	0.65	0.70
0.10	0.109	0.221	0.336	0.455	0.578	0.704	0.833	0.966	1.102	1.242	1.386	1.533	1.684	1.839
0.15	0.189	0.383	0.582	0.788	1.001	1.221	1.450	1.687	1.932	2.187	2.450	2.721	3.001	3.290
0.20	0.298	0.597	0.899	1.204	1.514	1.828	2.149	2.476	2.813	3.169	3.541	3.929	4.333	4.752
0.25	0.457	0.934	1.429	1.941	2.470	3.013	3.571	4.142	4.727	5.325	5.936	6.558	7.195	7.840
0.30	0.668	1.367	2.093	2.852	3.634	4.448	5.282	6.139	7.027	7.933	8.858	9.806	10.774	11.762
0.35	0.955	1.950	2.985	4.059	5.170	6.316	7.499	8.714	9.955	11.232	12.540	13.865	15.222	16.595
0.40	1.355	2.756	4.203	5.691	7.225	8.797	10.405	12.043	13.711	15.405	17.121	18.867	20.609	22.405
0.45	1.923	3.878	5.864	7.879	9.917	11.970	14.044	16.124	18.204	20.316	22.425	24.519	26.631	28.747
0.50	2.737	5.417	8.049	10.630	13.176	15.649	18.155	20.637	23.038	25.388	27.816	30.207	32.566	34.786
0.55	3.849	7.351	10.601	13.677	16.622	19.450	22.237	24.934	27.580	30.183	32.736	35.267	37.699	40.144
0.60	5.141	9.306	12.988	16.376	19.564	22.610	25.483	28.386	31.155	33.883	36.523	39.162	41.731	44.265
0.65	6.076	10.648	14.589	18.169	21.518	24.692	27.755	30.697	33.576	36.371	39.098	41.831	44.466	47.024
0.70	6.245	11.028	15.156	18.897	22.385	25.650	28.799	31.686	34.850	37.743	40.555	43.341	46.019	48.695

FIGURE 15

HARMONIC SWAY TEST: ALBERT MODEL: BOTH STRUTS FULLY EXTENDED: PREDICTED LOADS ON MDTF: towing speed = 4 m/s

force fy on lower bearing on forward lower strut (kN)

	ampl (m)													
f (hz)	0.05	0.10	0.15	0.20	0.25	0.30	0.35	0.40	0.45	0.50	0.55	0.60	0.65	0.70
0.10	0.734	1.490	2.269	3.072	3.897	4.746	5.620	6.517	7.437	8.382	9.352	10.345	11.361	12.404
0.15	1.275	2.582	3.926	5.313	6.750	8.237	9.780	11.380	13.037	14.751	16.526	18.357	20.245	22.194
0.20	2.007	4.026	6.062	8.122	10.211	12.336	14.497	16.701	18.980	21.380	23.892	26.509	29.235	32.059
0.25	3.086	6.302	9.642	13.097	16.662	20.326	24.091	27.947	31.888	35.928	40.046	44.245	48.539	52.895
0.30	4.508	9.221	14.121	19.239	24.518	30.008	35.633	41.419	47.405	53.517	59.763	66.159	72.686	79.350
0.35	6.445	13.157	20.140	27.383	34.878	42.613	50.592	58.786	67.163	75.777	84.603	93.541	102.694	111.956
0.40	9.141	18.594	28.353	38.397	48.746	59.351	70.196	81.252	92.502	103.927	115.506	127.284	139.039	151.159
0.45	12.973	26.166	39.565	53.158	66.904	80.757	94.748	108.783	122.813	137.064	151.291	165.420	179.669	193.939
0.50	18.466	36.544	54.303	71.713	88.892	105.576	122.482	139.227	155.423	171.283	187.658	203.790	219.704	234.682
0.55	25.967	49.593	71.518	92.270	112.141	131.218	150.021	168.219	186.069	203.627	220.852	237.932	254.336	270.835
0.60	34.681	62.784	87.627	110.484	131.986	152.540	171.924	191.509	210.191	228.592	246.404	264.207	281.541	298.637
0.65	40.992	71.839	98.428	122.575	145.174	166.583	187.246	207.101	226.520	245.378	263.777	282.215	299.991	317.245
0.70	42.132	74.400	102.251	127.490	151.024	173.050	194.293	213.772	235.114	254.633	273.602	292.403	310.467	328.522

bending moment mx on forward lower strut at lower bearing location (kN-m)

	ampl (m)													
f (hz)	0.05	0.10	0.15	0.20	0.25	0.30	0.35	0.40	0.45	0.50	0.55	0.60	0.65	0.70
0.10	0.109	0.221	0.336	0.455	0.578	0.704	0.833	0.966	1.102	1.242	1.386	1.533	1.684	1.839
0.15	0.189	0.383	0.582	0.788	1.001	1.221	1.450	1.687	1.932	2.187	2.450	2.721	3.001	3.290
0.20	0.298	0.597	0.899	1.204	1.514	1.828	2.149	2.476	2.813	3.169	3.541	3.929	4.333	4.752
0.25	0.457	0.934	1.429	1.941	2.470	3.013	3.571	4.142	4.727	5.325	5.936	6.558	7.195	7.840
0.30	0.668	1.367	2.093	2.852	3.634	4.448	5.282	6.139	7.027	7.933	8.858	9.806	10.774	11.762
0.35	0.955	1.950	2.985	4.059	5.170	6.316	7.499	8.714	9.955	11.232	12.540	13.865	15.222	16.595
0.40	1.355	2.756	4.203	5.691	7.225	8.797	10.405	12.043	13.711	15.405	17.121	18.867	20.609	22.405
0.45	1.923	3.878	5.864	7.879	9.917	11.970	14.044	16.124	18.204	20.316	22.425	24.519	26.631	28.747
0.50	2.737	5.417	8.049	10.630	13.176	15.649	18.155	20.637	23.038	25.388	27.816	30.207	32.566	34.786
0.55	3.849	7.351	10.601	13.677	16.622	19.450	22.237	24.934	27.580	30.183	32.736	35.267	37.699	40.144
0.60	5.141	9.306	12.988	16.376	19.564	22.610	25.483	28.386	31.155	33.883	36.523	39.162	41.731	44.265
0.65	6.076	10.648	14.589	18.169	21.518	24.692	27.755	30.697	33.576	36.371	39.098	41.831	44.466	47.024
0.70	6.245	11.028	15.156	18.897	22.385	25.650	28.799	31.686	34.850	37.743	40.555	43.341	46.019	48.695

maximum bending stress on forward lower strut (MPa)

	ampl (m)													
f (hz)	0.05	0.10	0.15	0.20	0.25	0.30	0.35	0.40	0.45	0.50	0.55	0.60	0.65	0.70
0.10	0.299	0.606	0.923	1.250	1.586	1.931	2.287	2.651	3.026	3.410	3.805	4.209	4.622	5.047
0.15	0.519	1.051	1.597	2.162	2.746	3.351	3.979	4.630	5.304	6.002	6.724	7.469	8.237	9.030
0.20	0.817	1.638	2.467	3.305	4.155	5.019	5.898	6.795	7.722	8.699	9.721	10.786	11.895	13.043
0.25	1.255	2.564	3.923	5.329	6.779	8.270	9.802	11.370	12.974	14.618	16.293	18.001	19.748	21.521
0.30	1.834	3.751	5.745	7.828	9.976	12.209	14.497	16.852	19.287	21.774	24.315	26.917	29.573	32.284
0.35	2.622	5.353	8.194	11.141	14.190	17.338	20.584	23.918	27.326	30.831	34.422	38.058	41.782	45.550
0.40	3.719	7.565	11.536	15.622	19.833	24.147	28.560	33.058	37.635	42.284	46.995	51.787	56.569	61.500
0.45	5.278	10.646	16.097	21.628	27.221	32.857	38.549	44.259	49.968	55.766	61.554	67.303	73.100	78.906
0.50	7.513	14.868	22.094	29.177	36.166	42.955	49.833	56.646	63.235	69.688	76.350	82.913	89.388	95.482
0.55	10.565	20.177	29.098	37.541	45.625	53.387	61.037	68.441	75.704	82.847	89.855	96.805	103.479	110.191
0.60	14.110	25.544	35.652	44.951	53.699	62.062	69.949	77.917	85.518	93.004	100.251	107.495	114.547	121.503
0.65	16.678	29.228	40.046	49.870	59.065	67.775	76.183	84.261	92.161	99.834	107.320	114.821	122.054	129.074
0.70	17.142	30.270	41.602	51.870	61.445	70.407	79.050	86.975	95.658	103.600	111.317	118.967	126.316	133.662

FIGURE 16

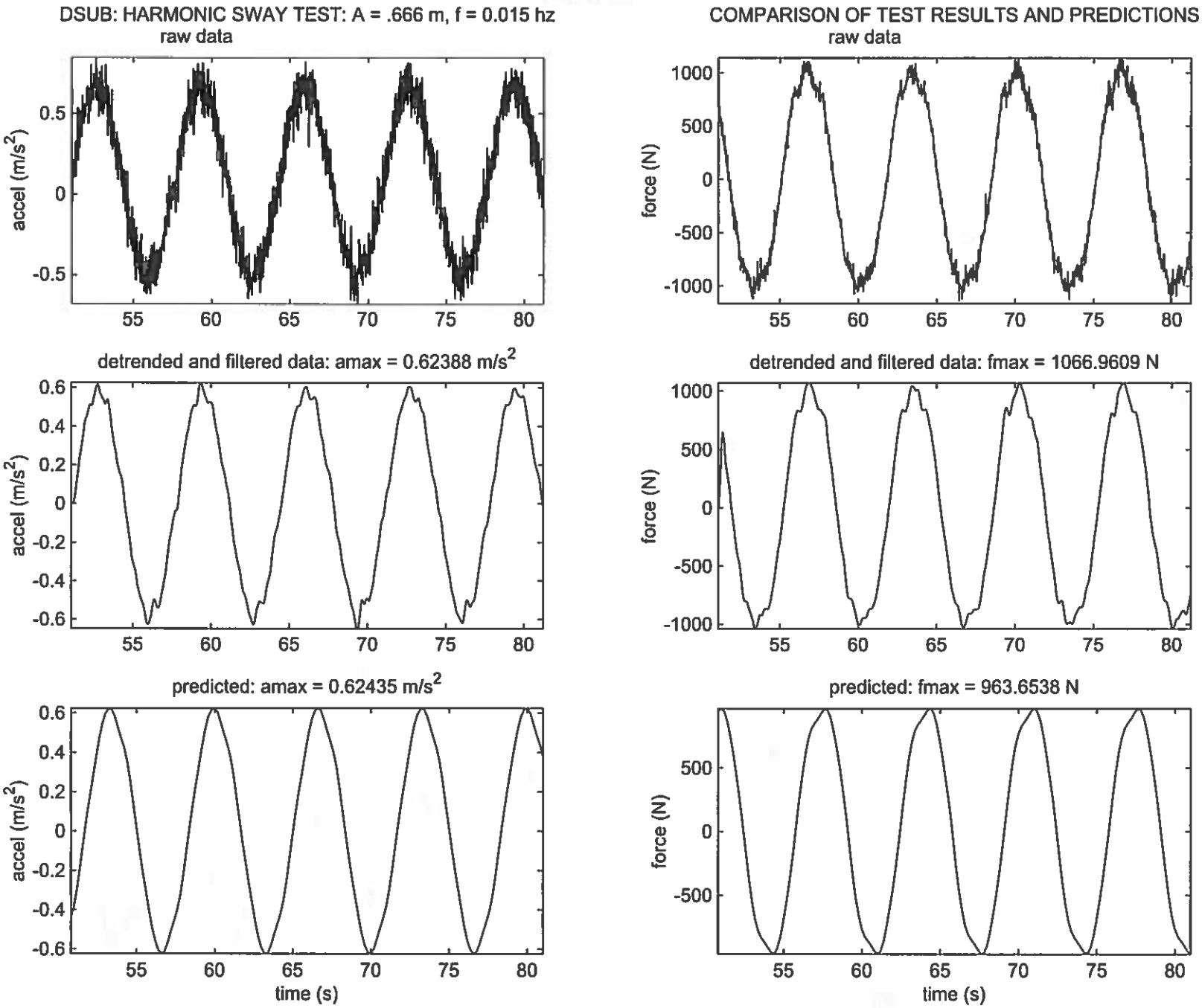
DSUB: HARMONIC SWAY TEST: A = .666 m, f = 0.015 hz
raw data
accel (m/s2)
detrended and filtered data: amax = 0.62388 m/s2
predicted: amax = 0.62435 m/s2
time (s)
COMPARISON OF TEST RESULTS AND PREDICTIONS
raw data
force (N)
detrended and filtered data: fmax = 1066.9609 N
predicted: fmax = 963.6538 N
time (s)

FIGURE 17

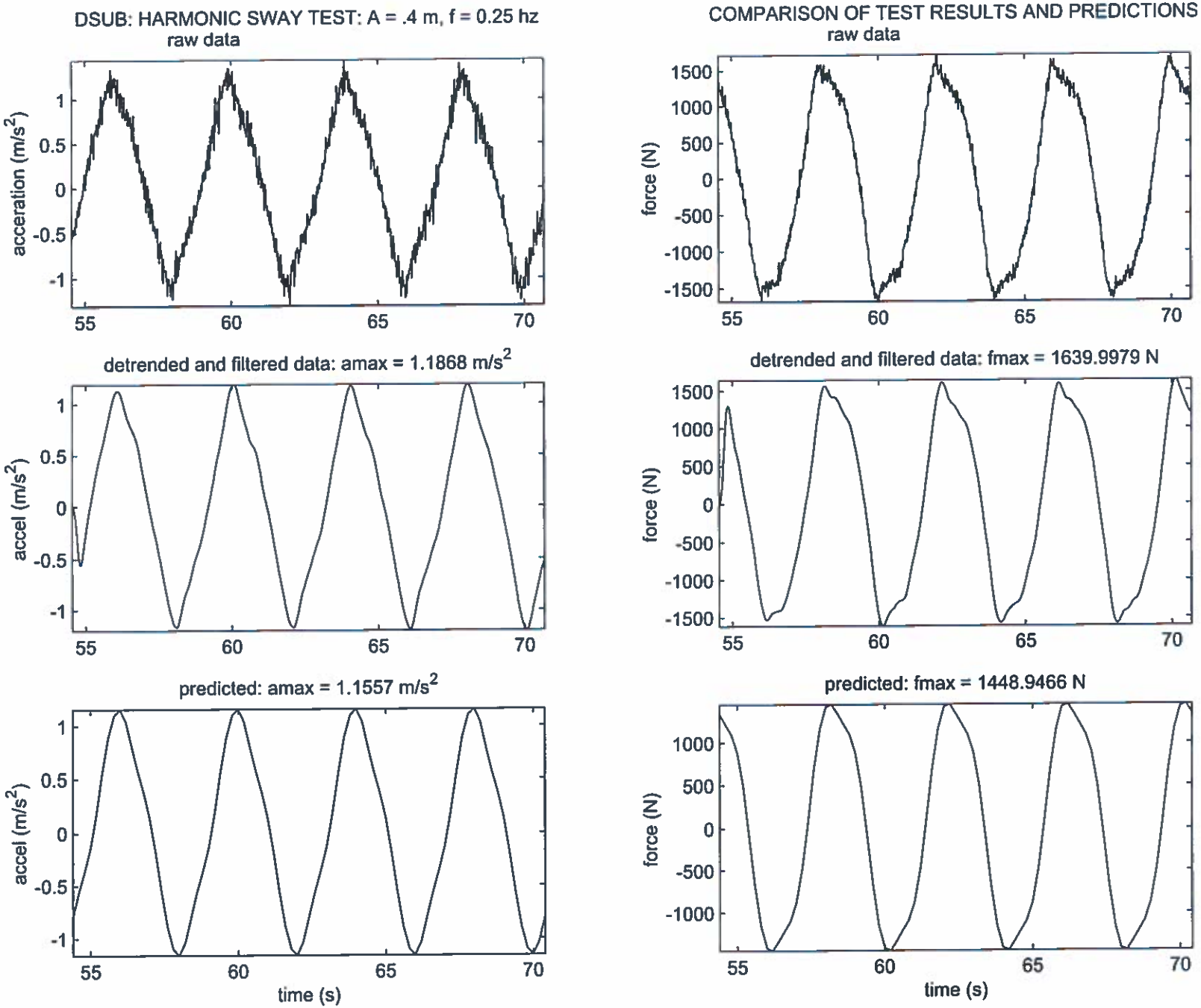
DSUB: HARMONIC SWAY TEST: A = .4 m, f = 0.25 hz
raw data
acceration (m/s2)
detrended and filtered data: amax = 1.1868 m/s2
accel (m/s2)
predicted: amax = 1.1557 m/s2
accel (m/s2)
time (s)
COMPARISON OF TEST RESULTS AND PREDICTIONS
raw data
force (N)
detrended and filtered data: fmax = 1639.9979 N
force (N)
predicted: fmax = 1448.9466 N
force (N)
time (s)

FIGURE 18

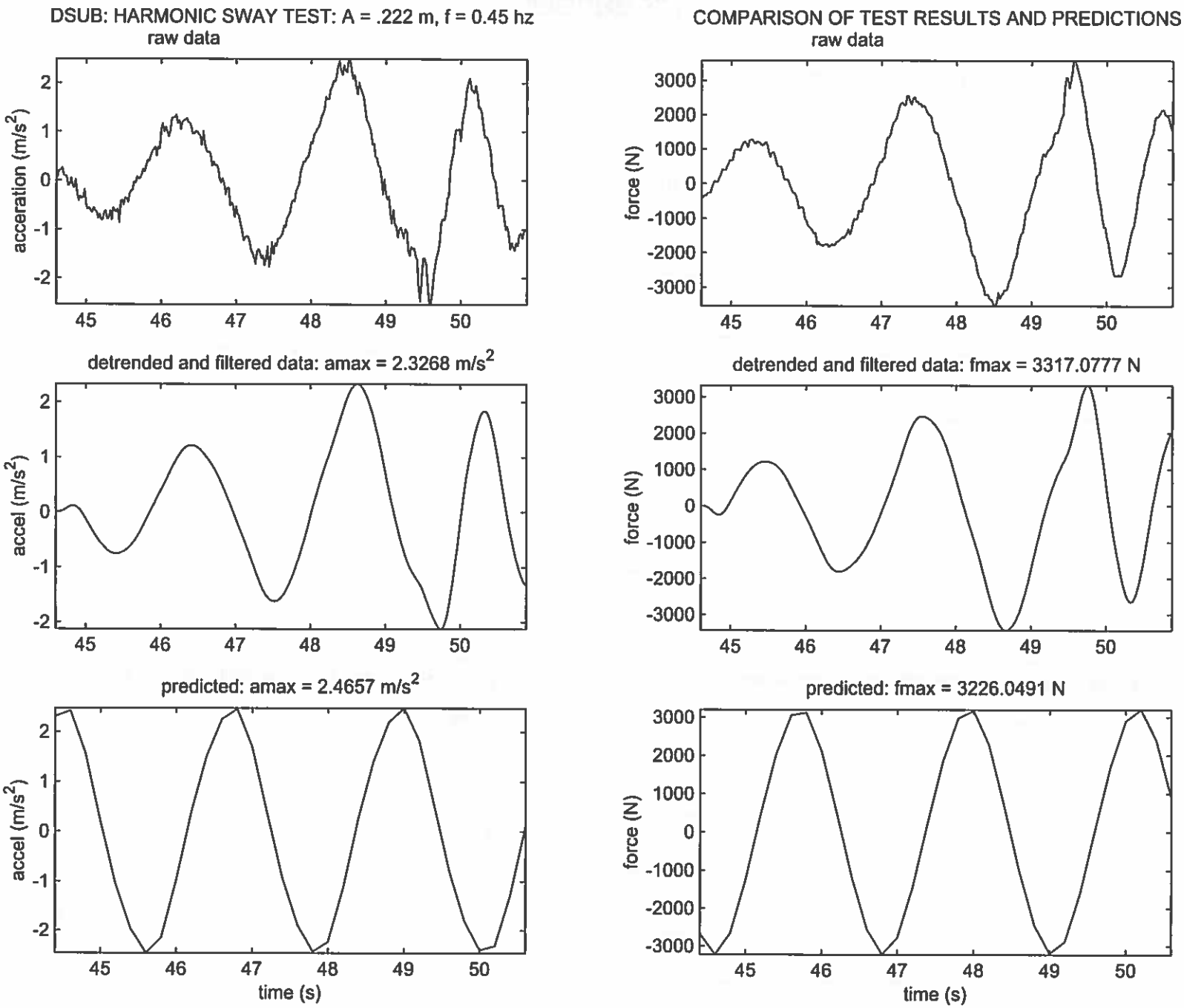
DSUB: HARMONIC SWAY TEST: A = .222 m, f = 0.45 hz
raw data
acceration (m/s2)
detrended and filtered data: amax = 2.3268 m/s2
accel (m/s2)
predicted: amax = 2.4657 m/s2
accel (m/s2)
time (s)
COMPARISON OF TEST RESULTS AND PREDICTIONS
raw data
force (N)
detrended and filtered data: fmax = 3317.0777 N
force (N)
predicted: fmax = 3226.0491 N
force (N)
time (s)

FIGURE 19

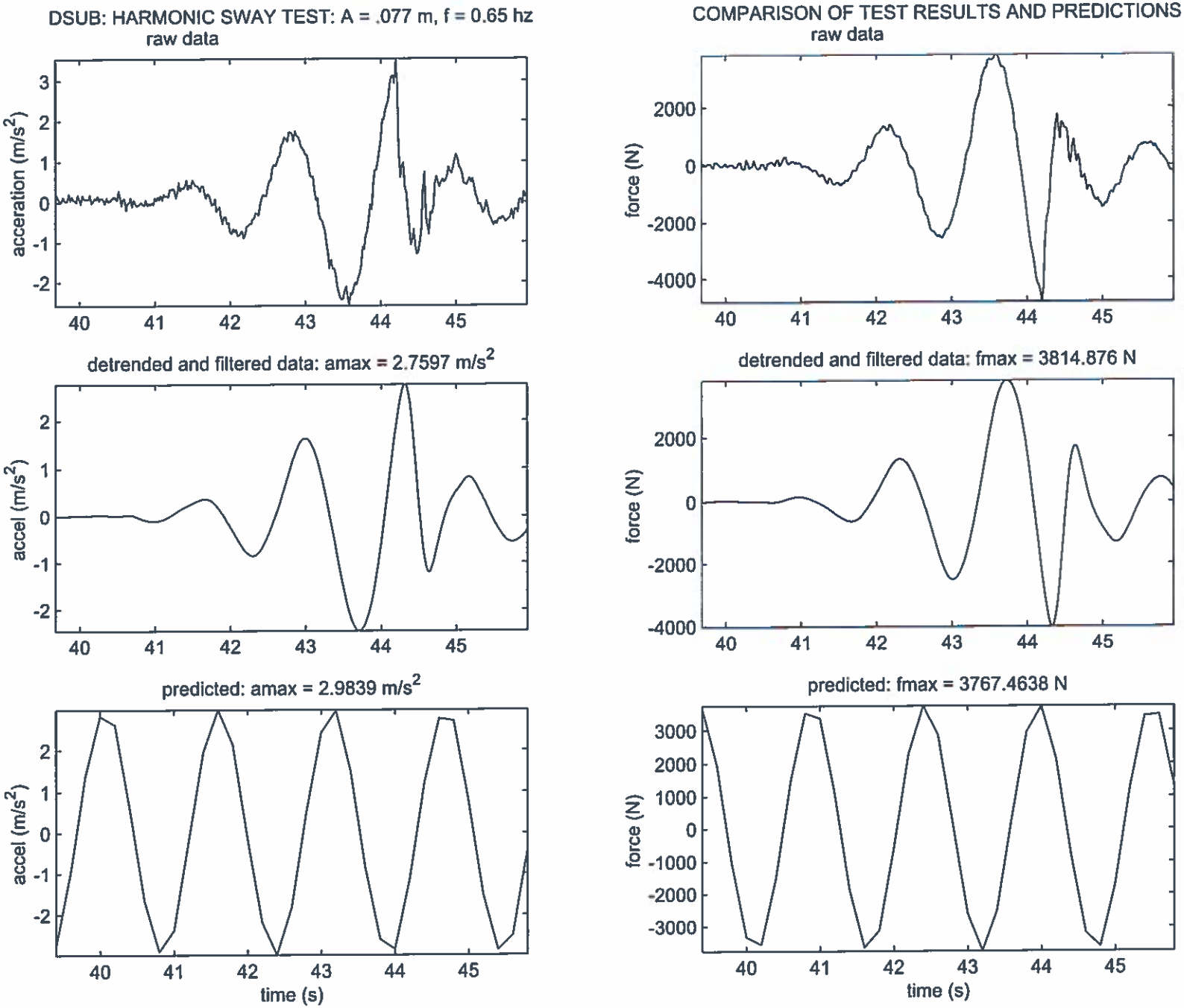
DSUB: HARMONIC SWAY TEST: A = .077 m, f = 0.65 hz
raw data
acceration (m/s2)
detrended and filtered data: amax = 2.7597 m/s2
accel (m/s2)
predicted: amax = 2.9839 m/s2
accel (m/s2)
time (s)
COMPARISON OF TEST RESULTS AND PREDICTIONS
raw data
force (N)
detrended and filtered data: fmax = 3814.876 N
force (N)
predicted: fmax = 3767.4638 N
force (N)
time (s)

FIGURE 20

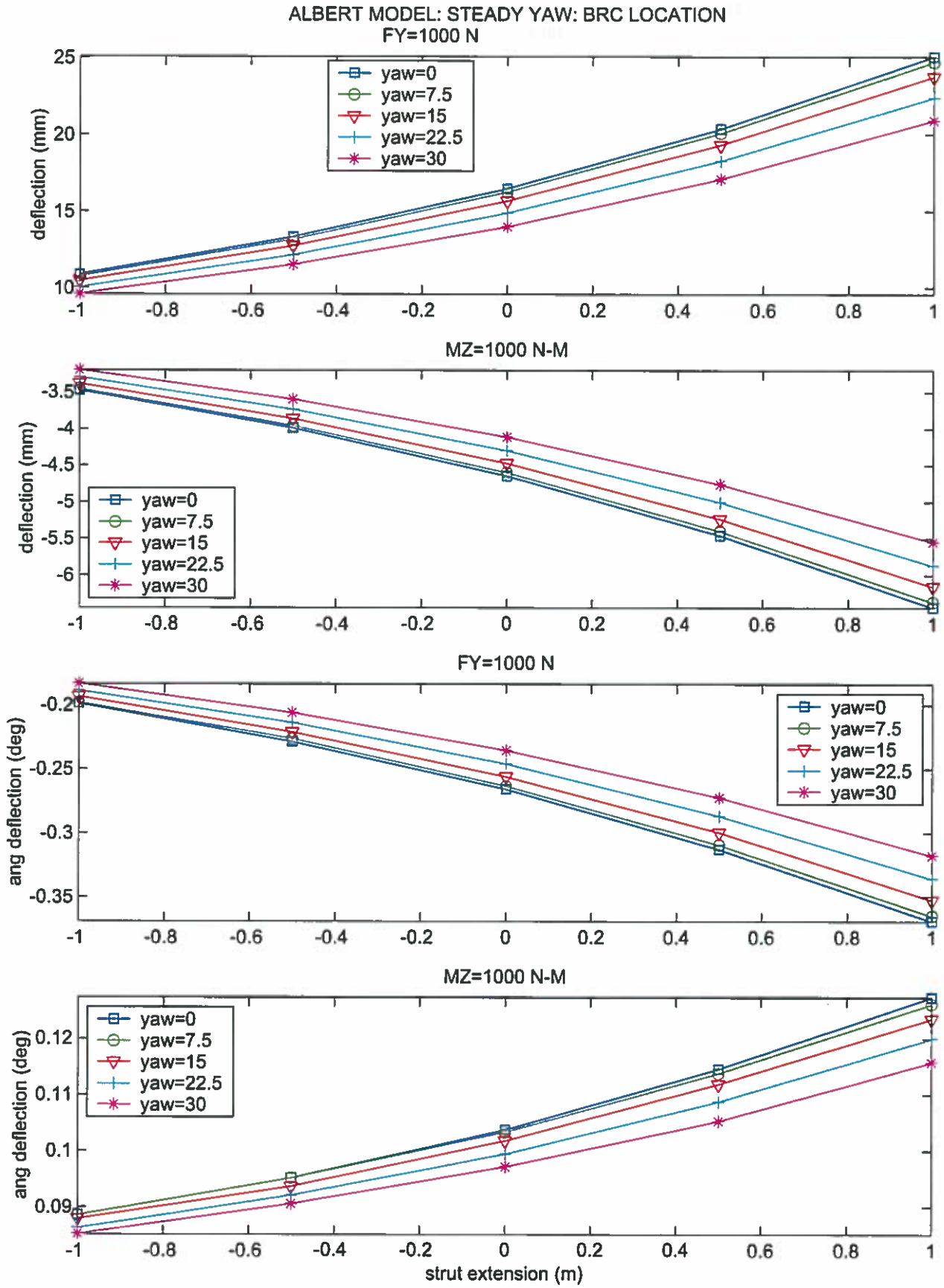

FIGURE 21
steady yaw deflections

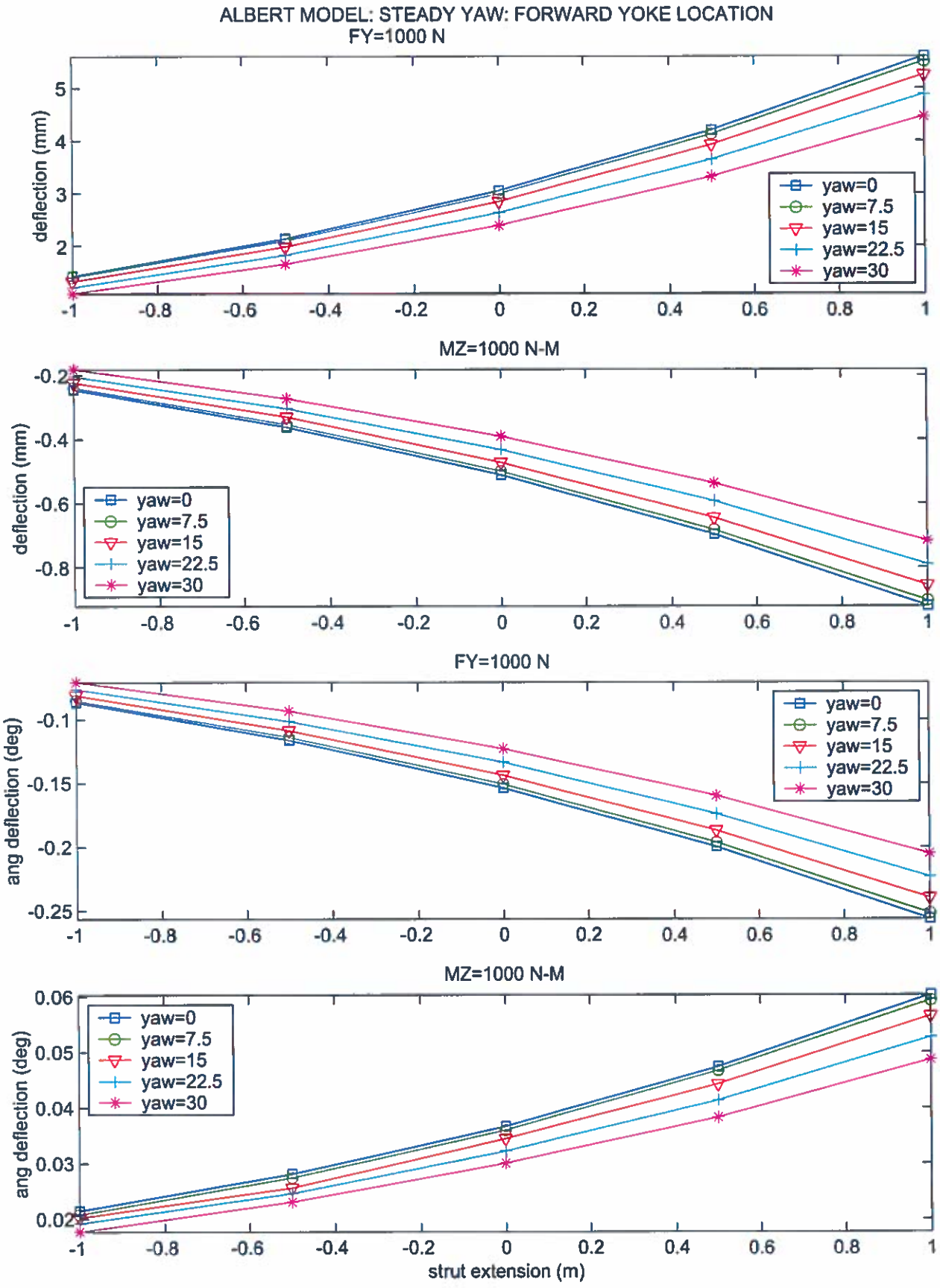

FIGURE 22
steady yaw deflections

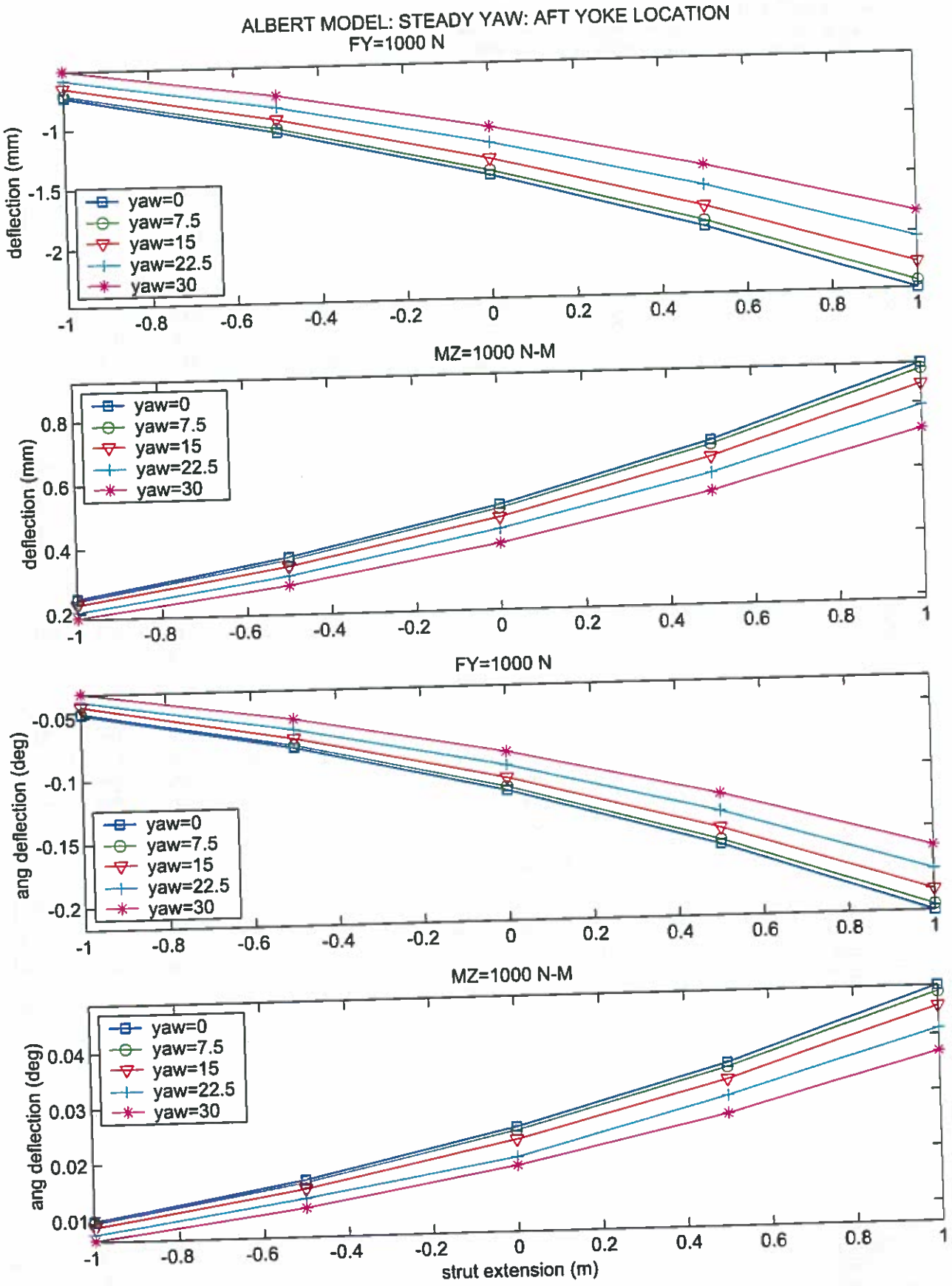

FIGURE 23
steady yaw deflections

deflections of sting at BRC, forward yoke, aft yoke: Albert configuration

load index 1 is fy=1000 N (positive in y-dirn)

load index 2 is mz=1000 N-m (positive counterclockwise in top view)

yaw angle is measured positive counterclockwise in top view

angular deflection is positive counterclockwise in top view

positive fy causes negative angular deflection so it decreases yaw angle if yaw angle positive

positive mz causes positive angular deflection so it increases yaw angle if yaw angle positive

strut ext is in metres; yaw is yaw angle in degrees

y2= deflection in y-direction (mm); y1=deflection at location dx aft of location of y2 (mm)

angle is angular deflection in degrees (positive counterclockwise)

angle = -180/pi*atan((y2-y1)/dx); dx (mm) = distance between locations of y2 and y1

					dx =	147.55		dx =	181.6		dx =	184
case	**load**	**strut**		**brc**		**fwd yoke**				**aft yoke**		
	index	**ext**	**yaw**	**y2**	**y1**	**angle**	**y2**	**y1**	**angle**	**y2**	**y1**	**angle**
e-10y00fy	1	-1	0	10.854	10.342	-0.1988	1.422	1.148	-0.0864	-0.728	-0.88	-0.0473
e-10y00mz	2	-1	0	-3.477	-3.249	0.0885	-0.245	-0.177	0.0215	0.2453	0.2767	0.0098
e-05y00fy	1	-0.5	0	13.304	12.715	-0.2287	2.13	1.762	-0.1161	-1.051	-1.297	-0.0766
e-05y00mz	2	-0.5	0	-3.992	-3.747	0.0951	-0.362	-0.273	0.0281	0.3628	0.4158	0.0165
e-00y00fy	1	0	0	16.439	15.754	-0.2660	3.046	2.559	-0.1537	-1.447	-1.814	-0.1143
e-00y00mz	2	0	0	-4.648	-4.381	0.1037	-0.512	-0.396	0.0366	0.5124	0.593	0.0251
e+05y00fy	1	0.5	0	20.341	19.535	-0.3130	4.197	3.563	-0.2000	-1.921	-2.438	-0.1610
e+05y00mz	2	0.5	0	-5.461	-5.166	0.1146	-0.698	-0.548	0.0473	0.6979	0.8126	0.0357
e+10y00fy	1	1	0	25.085	24.134	-0.3693	5.61	4.797	-0.2565	-2.477	-3.175	-0.2173
e+10y00mz	2	1	0	-6.446	-6.118	0.1274	-0.922	-0.731	0.0603	0.9225	1.079	0.0487
e-10y75fy	1	-1	7.5	10.743	10.233	-0.1980	1.393	1.124	-0.0849	-0.707	-0.854	-0.0458
e-10y75mz	2	-1	7.5	-3.453	-3.225	0.0885	-0.239	-0.173	0.0208	0.2397	0.27	0.0094
e-05y75fy	1	-0.5	7.5	13.146	12.563	-0.2264	2.089	1.728	-0.1139	-1.022	-1.262	-0.0747
e-05y75mz	2	-0.5	7.5	-3.958	-3.713	0.0951	-0.354	-0.267	0.0274	0.3549	0.4064	0.0160
e-00y75fy	1	0	7.5	16.227	15.548	-0.2637	2.99	2.512	-0.1508	-1.409	-1.767	-0.1115
e-00y75mz	2	0	7.5	-4.602	-4.336	0.1033	-0.501	-0.387	0.0360	0.5018	0.5804	0.0245
e+05y75fy	1	0.5	7.5	20.064	19.267	-0.3095	4.124	3.501	-0.1966	-1.873	-2.379	-0.1576
e+05y75mz	2	0.5	7.5	-5.401	-5.108	0.1138	-0.684	-0.536	0.0467	0.6841	0.7963	0.0349
e+10y75fy	1	1	7.5	24.732	23.792	-0.3650	5.516	4.717	-0.2521	-2.418	-3.101	-0.2127
e+10y75mz	2	1	7.5	-6.369	-6.044	0.1262	-0.905	-0.717	0.0593	0.9051	1.058	0.0476
e-10y15fy	1	-1	15	10.441	9.942	-0.1938	1.316	1.059	-0.0811	-0.653	-0.787	-0.0417
e-10y15mz	2	-1	15	-3.387	-3.161	0.0878	-0.224	-0.16	0.0202	0.2246	0.2521	0.0086
e-05y15fy	1	-0.5	15	12.72	12.15	-0.2213	1.978	1.634	-0.1085	-0.946	-1.169	-0.0694
e-05y15mz	2	-0.5	15	-3.864	-3.623	0.0936	-0.33	-0.249	0.0256	0.3336	0.3812	0.0148
e-00y15fy	1	0	15	15.649	14.989	-0.2563	2.839	2.383	-0.1439	-1.309	-1.644	-0.1043
e-00y15mz	2	0	15	-4.476	-4.214	0.1017	-0.473	-0.364	0.0344	0.4731	0.5464	0.0228
e+05y15fy	1	0.5	15	19.307	18.535	-0.2998	3.923	3.33	-0.1871	-1.746	-2.221	-0.1479
e+05y15mz	2	0.5	15	-5.237	-4.949	0.1118	-0.646	-0.506	0.0442	0.6467	0.7519	0.0328
e+10y15fy	1	1	15	23.767	22.858	-0.3530	5.257	4.496	-0.2401	-2.259	-2.904	-0.2008
e+10y15mz	2	1	15	-6.16	-5.842	0.1235	-0.857	-0.678	0.0565	0.8574	1.002	0.0450
e-10y225fy	1	-1	22.5	10.03	9.544	-0.1887	1.208	0.9671	-0.0760	-0.581	-0.699	-0.0367
e-10y225mz	2	-1	22.5	-3.297	-3.075	0.0862	-0.204	-0.143	0.0192	0.2041	0.2279	0.0074
e-05y225fy	1	-0.5	22.5	12.133	11.582	-0.2140	1.823	1.502	-0.1013	-0.846	-1.046	-0.0623
e-05y225mz	2	-0.5	22.5	-3.737	-3.5	0.0920	-0.304	-0.226	0.0246	0.3045	0.3468	0.0132
e-00y225fy	1	0	22.5	14.849	14.215	-0.2462	2.624	2.201	-0.1335	-1.177	-1.48	-0.0944
e-00y225mz	2	0	22.5	-4.303	-4.047	0.0994	-0.433	-0.331	0.0322	0.4366	0.4997	0.0196
e+05y225fy	1	0.5	22.5	18.252	17.513	-0.2870	3.638	3.086	-0.1742	-1.577	-2.01	-0.1348
e+05y225mz	2	0.5	22.5	-5.009	-4.729	0.1087	-0.594	-0.463	0.0413	0.5948	0.6905	0.0298
e+10y225fy	1	1	22.5	22.412	21.547	-0.3359	4.887	4.179	-0.2234	-2.048	-2.64	-0.1843
e+10y225mz	2	1	22.5	-5.87	-5.561	0.1200	-0.791	-0.624	0.0527	0.7911	0.9229	0.0410
e-10y30fy	1	-1	30	9.59	9.117	-0.1837	1.09	0.8658	-0.0707	-0.509	-0.61	-0.0315
e-10y30mz	2	-1	30	-3.202	-2.983	0.0850	-0.182	-0.126	0.0177	0.1824	0.2022	0.0062
e-05y30fy	1	-0.5	30	11.499	10.968	-0.2062	1.65	1.354	-0.0934	-0.746	-0.92	-0.0542
e-05y30mz	2	-0.5	30	-3.601	-3.368	0.0905	-0.273	-0.2	0.0230	0.2734	0.31	0.0114
e-00y30fy	1	0	30	13.977	13.37	-0.2357	2.384	1.994	-0.1230	-1.044	-1.313	-0.0838
e-00y30mz	2	0	30	-4.116	-3.866	0.0971	-0.391	-0.296	0.0300	0.391	0.4492	0.0181
e+05y30fy	1	0.5	30	17.093	16.391	-0.2726	3.315	2.808	-0.1600	-1.405	-1.793	-0.1208
e+05y30mz	2	0.5	30	-4.762	-4.491	0.1052	-0.538	-0.417	0.0382	0.5384	0.6237	0.0266
e+10y30fy	1	1	30	20.915	20.096	-0.3180	4.465	3.814	-0.2054	-1.834	-2.367	-0.1660
e+10y30mz	2	1	30	-5.552	-5.254	0.1157	-0.718	-0.564	0.0486	0.7185	0.837	0.0369

FIGURE 24: steady yaw deflections

TOP VIEW OF STING

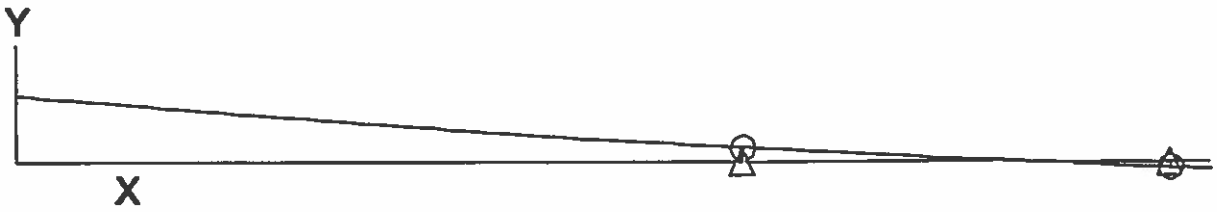

DEFLECTED SHAPE DUE TO FY

Note: The Z axis is positive out of the page

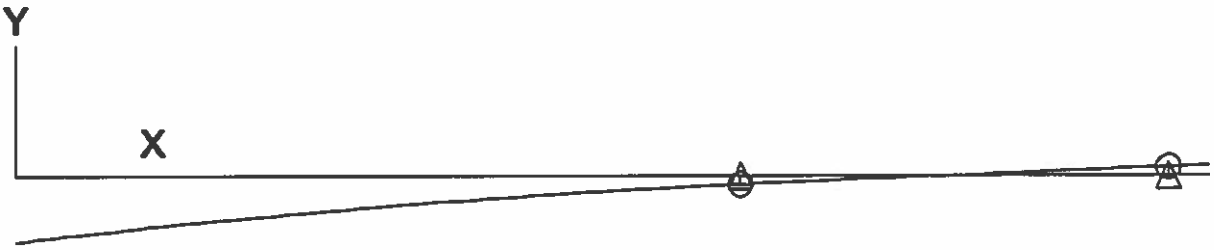

DEFLECTED SHAPE DUE TO MZ

FIGURE 25: deflected shapes of sting